Recent Innovations in Satellite-Based Applications and their Impacts on Tropical Cyclone Analyses and Forecasts

Christopher Velden[1], John Knaff [2], Derrick Herndon[1], Alexis Mouche[3], Jeffrey Hawkins[1], Giulia Panegrossi[4], Ad Stoffelen[5], Joseph Courtney[6], Taiga Tsukada[7], Anne-Claire Fontan[8]

[1] Cooperative Institute for Meteorological Satellite Studies (CIMSS), University of Wisconsin, Madison, WI, USA
[2] NOAA/NESDIS Regional and Mesoscale Meteorological Branch (RAMMB), Fort Collins, CO, USA
[3] Institut Francais de Recherche pour l'Exploitation de la Mer (IFREMER), Plouzane, France
[4] National Research Council of Italy, Institute of Atmospheric Sciences and Climate (CNR-ISAC), Rome, Italy
[5] Royal Netherlands Meteorological Institute (KNMI), De Bilt, Netherlands
[6] Bureau of Meteorology (BOM), Perth, Australia
[7] Cooperative Institute for Research in the Atmosphere (CIRA), Colorado State University, Fort Collins, CO, USA
[8] WMO, Tropical Cyclone Programme (TCP), Geneva, Switzerland

Corresponding author: C. Velden chrisv@ssec.wisc.edu

Abstract

Tropical cyclones (TCs) are a global extreme weather hazard well known for their occasional devastating impacts on life and property, as well as ecological systems. As human populations and infrastructure built along coastlines grow, they are increasingly prone to threats from landfalling TCs. These storms spend most of their lifecycle over oceanic basins, thus satellite-based reconnaissance is crucial for monitoring and analyzing key TC behavioral attributes critical to the forecast process. This article presents an overview of some of the recent advances in meteorological satellite capabilities to observe TCs, along with emerging techniques to analyze the data into TC-focused diagnostic products. We also devote a section on satellite applications to TC-like storms in the Mediterranean Sea, coined 'Medicanes'. Finally, we present a peek at emerging geosynchronous equatorial orbit and low Earth orbiting satellites and sensors that have recently been deployed or will be in the near future by multiple nations and commercial entities that should further benefit TC (and Medicane) analysis and forecasting.

Keywords
Satellite applications
Tropical Cyclones
Medicanes

1. Introduction

Tropical cyclones (also known regionally as hurricanes, typhoons, and cyclones; we refer to them as TCs in this paper) represent simultaneously one of nature's most wondrous creations and formidable threats. While mainly developing in the tropics, these tempests can result in significant losses of life and property even as they sometimes traverse into the higher latitudes such as Western Europe, Northeast Asia and eastern North America. Medicanes (*Medi*terranean tropical-like hurri*canes*) are sometimes destructive Mediterranean Sea area cyclones with thermal and wind structural characteristics that resemble those of TCs. Early and continuous monitoring of these extreme weather events can lead to crucial warnings in advance of their potentially disruptive and deadly consequences and help to reduce societal impacts.

The detection of these storms has been greatly improved by the advent and surveillance capabilities of meteorological satellites. Regarding TCs, a constellation of geostationary (GEO) and low Earth-orbiting (LEO) platforms routinely scans the global tropics with increasing frequency and ever-improving sensors. A myriad of multispectral imagery qualitatively tracks and catalogs the genesis, evolution, and dissipation of these cyclones. In the absence of TC-penetrating reconnaissance aircraft surveillance and other in-situ observations, global TC forecast centers primarily rely on satellite-based remote sensing methods to determine TC position, intensity and size (radii of gale, storm and hurricane force surface winds). More recently, the TC research and development community has taken advantage of space-borne sensors with improved spatial, spectral and temporal sampling along with increasing computer capacity and sophisticated analysis techniques to create automated TC-focused products and displays that can provide near-real-time data and guidance that supplements standard human imagery interpretation. We have come a long way from the early days of satellites and the primitive ways in which their data were used for TC analysis (Fig. 1).

Recognition of this progress amongst the global TC community led to the establishment of the World Meteorological Organization (WMO) International Workshops on the Satellite Analysis of Tropical Cyclones (IWSATC), held every 3-5 years. The main purpose of the IWSATC is to share the latest knowledge and techniques developed by the research community with operational forecasters of the international TC warning centers. For more details on the material highlighted in this paper and additional satellite-based TC applications, see the WMO IWSATC website at https://community.wmo.int/en/international-workshop-satellite-analysis-tropical-cyclones-iwsatc

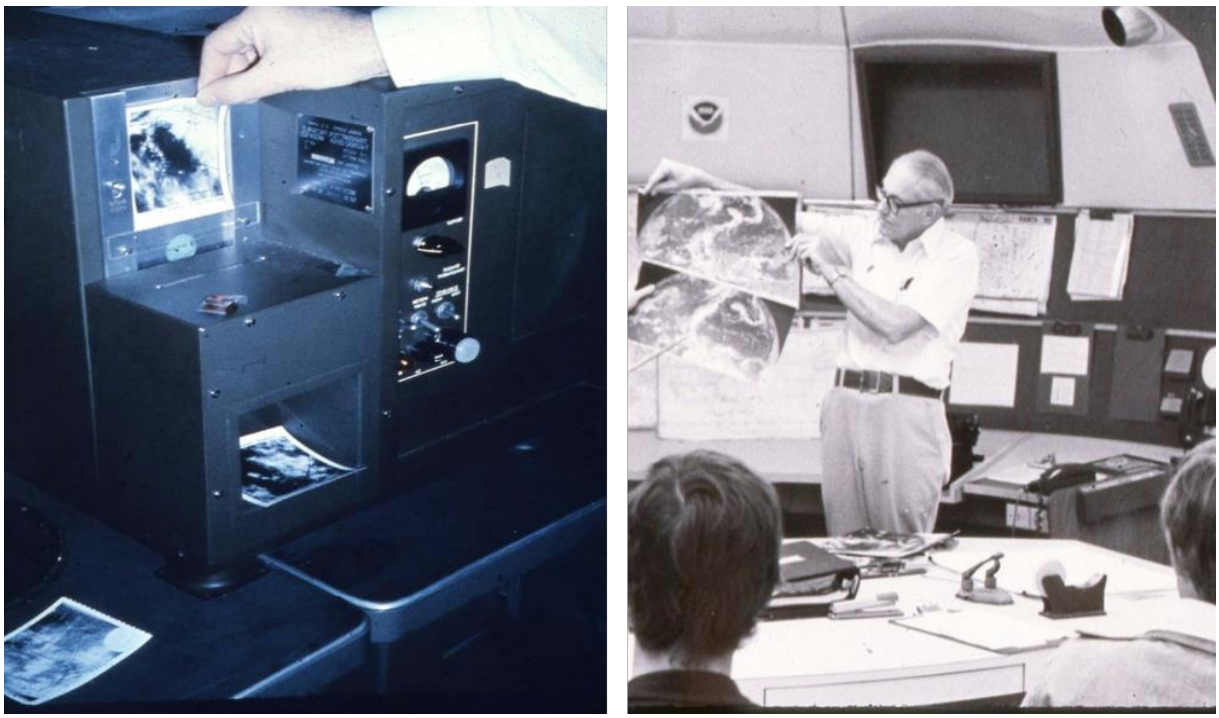

Fig. 1: With the arrival of TIROS, NIMBUS and GOES satellites in the 1960s and 70s, forecasters at the U.S. National Hurricane Center acquired important new analysis tools. Satellite images were initially transmitted via phone lines and received on a special image processor (left) and later via facsimile for use in daily tropical discussions (right). [Images courtesy NOAA/NHC]

Medicanes are cyclones that occasionally occur over the Mediterranean Sea exhibiting phenomenological features typical of tropical (or sub-tropical) cyclones, such as a warm thermal core profile, a cloud free eye surrounded by spiraling rain bands around the center, strong surface winds near the center, and heavy precipitation (Lagouvardos et al., 1999; Reale and Atlas, 2001). They usually originate from extra-tropical cyclones, when baroclinic processes are driving the development and intensification (e.g., Miglietta et al., 2017; Flaounas et al., 2021). During their evolution, they undergo a so-called *tropical transition* (Davis and Bosart, 2003; Miglietta and Rotunno, 2019), and often cause floods, storm surges and fierce winds leading to social disruption and sometimes casualties. For example, the most intense Medicane on record is Ianos that swept across the Ionian Sea (a sub-basin of the Mediterranean Sea) in 2020 (Lagouvardos et al., 2022). During its peak intensity (equivalent to a category 1 hurricane), torrential rainfall and severe wind gusts affected southern Italy, the western coast of Greece and the Ionian Islands. Since Medicanes spend most of their lifecycle over a marine environment and away from conventional land-based observations, satellite remote sensing is crucial to their analysis and forecast.

The first sections of this article highlight recent ways in which various satellite platforms and sensors are providing novel information to the TC and Medicane operational and research communities, and their impacts on the analysis and forecast process. The article then offers a glimpse to the future, as technological advancements are enabling much smaller and more cost-effective satellite-based alternatives to observing the troposphere that likely will result in constellations that provide unprecedented sampling of these extreme weather events. Note: Given the large volume of acronyms in this review paper, readers can refer to the list in Appendix B.

2. TC applications from new-generation geostationary satellites

Over the past five decades, geostationary meteorological satellites have formed the basis for global monitoring of TC development, location, motion and cloud structure with their predictable low-latency and rapid sampling interval visible (VIS) and infrared (IR) imagery. As digitized data and animation capabilities became available (e.g., McIDAS (Lazzara et al., 1990); AWIPS (Tuell et al., 2008)), the value of the imagery took on an even greater importance. As quoted by the Director of the U.S. National Hurricane Center (NHC) Dr. Robert Sheets (Sheets, 1990):

> "***The greatest single advancement in observing tools for tropical meteorology was unquestionably the advent of the geosynchronous meteorological satellite. If there was a choice of only one observing tool for use in meeting the responsibilities of the NHC, the author would clearly choose the geosynchronous satellite with its present day associated accessing, processing and displaying systems available at NHC.***"

Geostationary satellites continue to evolve, as the second and today's third-generation imagers provide higher spatiotemporal resolution, increased spectral resolution, and more precise pixel geolocation. The results are stunning presentations of storm tracks, circulating eye features, and even lightning activity. Figures 2 and 3 show examples of Hurricane Milton (2024) as it threatened Florida as viewed from the U.S. GOES-EAST Advanced Baseline Imager (ABI) meso-sector scans at 1-min. intervals. Similar rapid-scanning capabilities (1 to 5 min. imaging intervals) are now available from the 2nd and 3rd generation European Meteosat series (MSG/MTG), Japan's recent Himawari series, Korea's GEO-KOMPSAT-2 series, India's INSAT series, and China's FengYun-4 (FY-4) series. Figure 2 also shows lightning activity from the GOES Geostationary Lightning Mapper, which has been correlated with TC intensity behavior (Stephenson et al., 2018; Slocum et al., 2023). This capability also now exists on the FY-4 and MTG satellite instrument payloads.

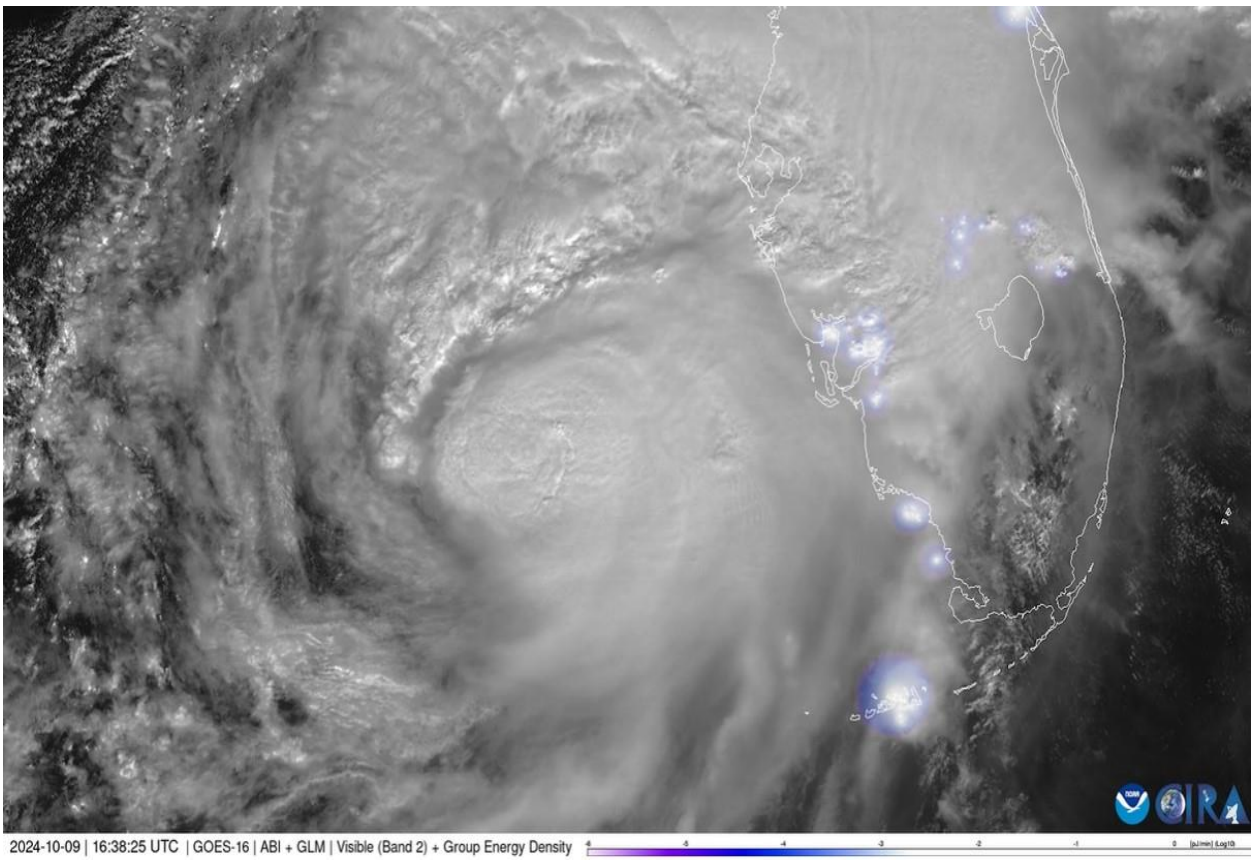

Fig 2. Hurricane Milton approaches Florida, U.S. on October 9, 2024, as viewed from GOES-East 1-minute interval Advanced Baseline Imager visible channel imagery. Also shown are lightning flashes (group energy density) via the GOES Lightning Mapper instrument. [Image/animation courtesy NOAA/CIRA]

Animated sequence:
https://satlib.cira.colostate.edu/wp-content/uploads/sites/23/2024/10/20241009150028-20241009201155_g16_meso_band2glm_milton-hits-florida_labels.mp4

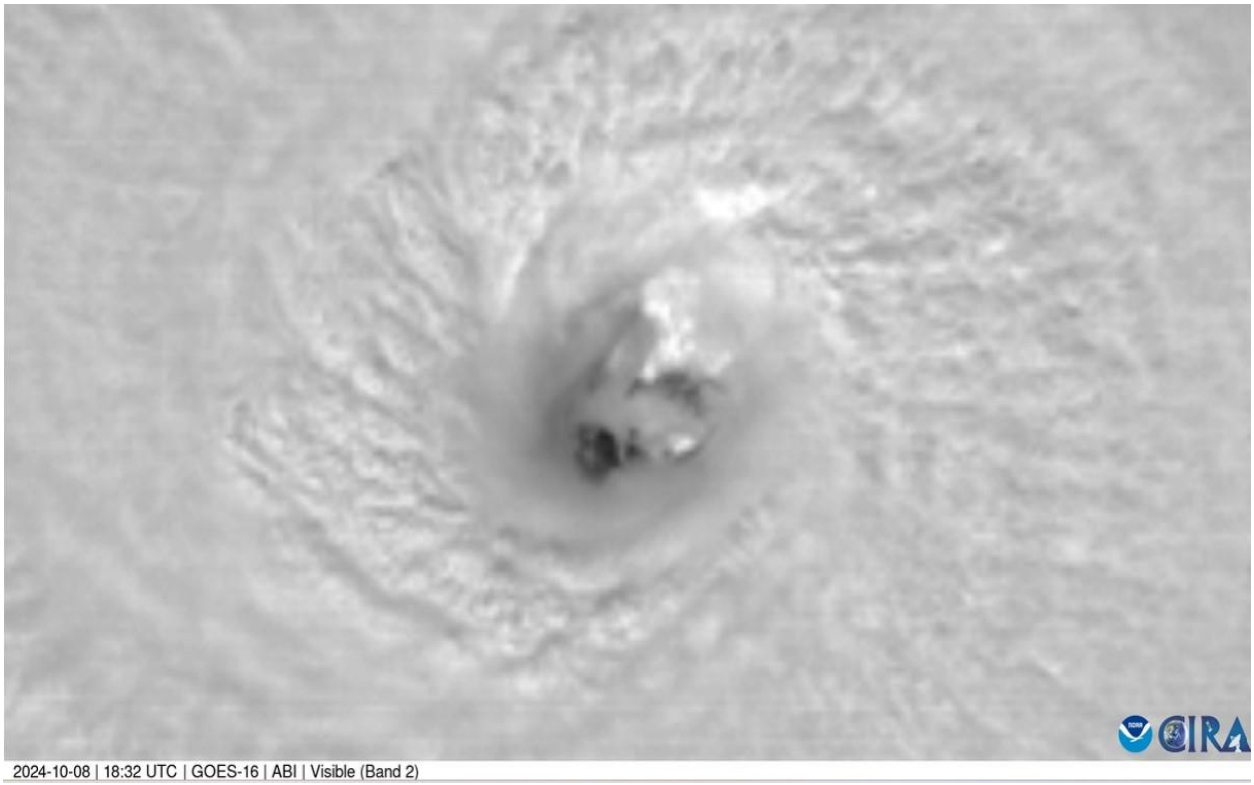

Fig 3. A close-up view of Hurricane Milton's eye on October 8, 2024, as viewed from GOES-EAST 1-minute meso-sector scan visible imagery. [Image/animation courtesy NOAA/CIRA]

Animated sequence:
https://satlib.cira.colostate.edu/wp-content/uploads/sites/23/2024/10/20241008183055-20241008211455_g16_meso_band2_milton-clear-cat-5-eye-ZOOM_labels.mp4

2.1. Derived GEO imager products

In recent years, the data from the advanced imagers in tandem with rapidly growing computing capacity have led to many novel applications that provide tailored imagery products and derived quantities designed to assist the analysis of TCs even further. Today's multispectral imagers with water vapor channels and the emissivity and reflectivity of the visible and near-IR channels can provide novel derived imagery products. These include, but are not limited to, the documentation of a TC diurnal convective signal that can be related to TC size and intensity changes (Dunion et al., 2014; Ditchek et al., 2019; Knaff et al., 2019); split-window imagery that identifies and tracks dry and dusty Saharan air layers as they traverse the Atlantic Ocean which can act to suppress TC activity (Dunion and Velden, 2004); depiction of airmass differences that can inform TC forecasters about impending extratropical transition (Goodman et al., 2012); tropical overshooting tops which are a proxy for TC convective vigor and intensity (Olander and Velden, 2009; Griffin, 2017); proxy nighttime visible imagery that can better detect the low-level circulation in sheared TCs for improved center-fixing applications (Chirokova et al., 2023); and most recently, synthetic microwave imagery from GEO that can simulate the TC convective structure and evolution (Haynes et al., 2022). Figure 4 illustrates some examples. Each product better informs forecasters and researchers about TC structure and/or near-environmental conditions that could impact the storm behavior.

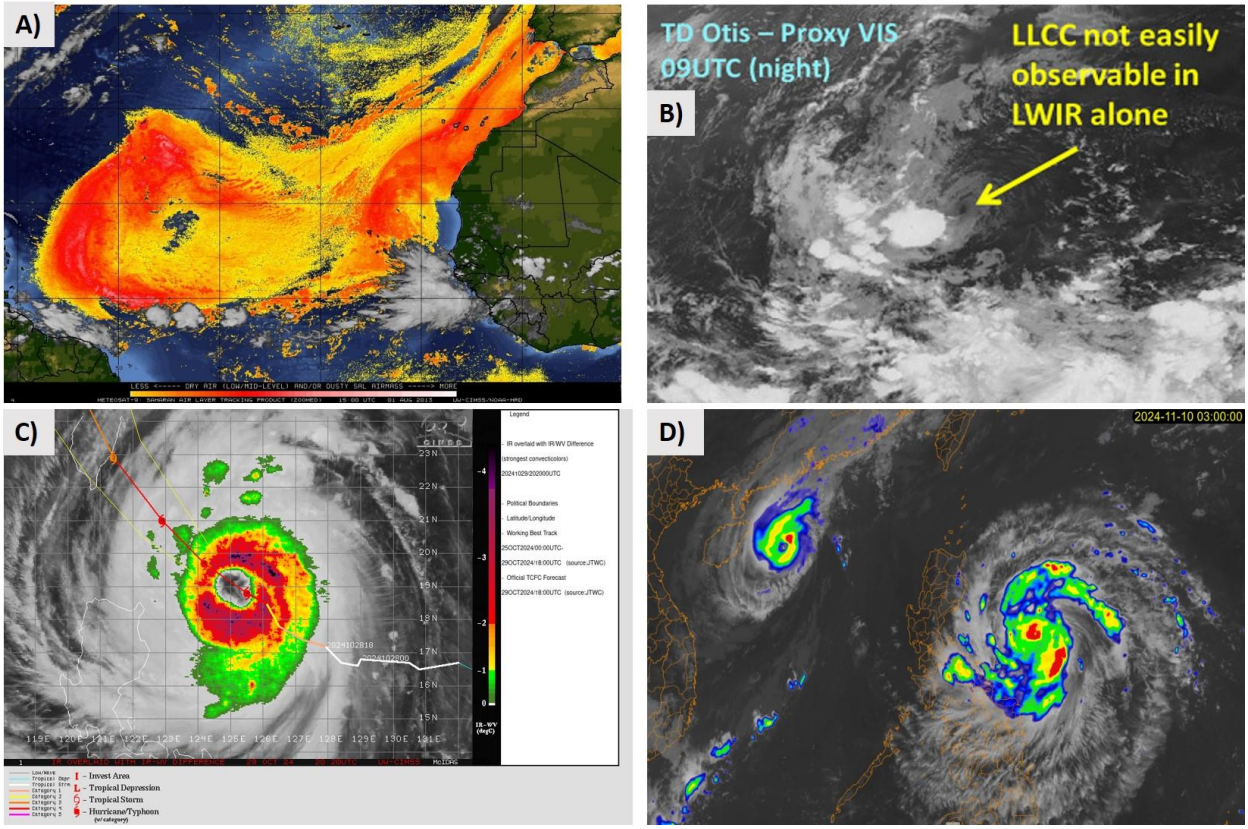

Fig. 4. Examples of derived GEO imagery tailored to TC environments. A) Meteosat-9 split-window depiction of a dusty and dry Saharan air layer surge (orange and yellows) over the Atlantic Ocean on 01 August 2013 (credit: Jason Dunion, CIMAS & CIMSS). B) Proxy-VIS nighttime image showing the low-level circulation center (LLCC) of TC Otis on 22 Aug. 2023 (credit: CIRA). C) Eyewall overshooting convective cloud tops (colors) obtained by differencing the Himawari-9 IR-window and 6.2-μm water vapor channel Tb (deg. C) during Typhoon Kong-rey on 29 Oct. 2024 (credit: CIMSS). D) Synthetic 89-GHz image from Himawari-9 AHI overlaid upon IR during Typhoon Yinxing (upper left) and Tropical Storm Toraji (center) on 10 Nov. 2024 (credit: Kathy Haynes, CIRA).

2.2. TC intensity estimation from GEO

Global operational forecast offices and WMO mandated Regional Specialized Meteorological Centers (RSMCs) heavily rely on satellite-based estimates of TC intensity for real-time monitoring and when conducting post-analyses of "final best tracks" (historical records of TC track and intensity). The empirical Dvorak technique (Dvorak, 1975, 1984) relies mainly on analysis of cloud patterns in IR and VIS imagery to infer TC intensity and is utilized globally as the predominant satellite-based procedure. The practical appeal and demonstrated skill in the face of tremendous dynamic complexity place the Dvorak technique for estimating TC intensity from satellites amongst the greatest meteorological innovations of our time (Velden et al., 2006). It has also been an important input tool for our highly valuable TC archives. The method does a reasonable job in most cases, however it is not without limitations and can depend somewhat on analyst judgement. When developing his technique, Dvorak did not have the full complement of satellite capabilities nor ground truth data that exist today, leading to inherent biases in the

empirically driven method's estimates, particularly notable at the very strong end of the TC intensity spectrum (Knaff et al., 2010).

The emergence of digital data and computer algorithms prompted efforts to automate and advance the Dvorak technique. Early efforts were somewhat crude (Zehr, 1989; Velden et al. 1998), but eventually culminated in the fully automated Advanced Dvorak Technique (ADT; Olander and Velden, 2007, 2019). The ADT is an objective approach that builds on the principles of the Dvorak technique, enhanced by rigorous statistical analysis and additional capabilities that exploit the improved qualities of satellite data available today. The ADT now runs operationally at the NOAA/NESDIS Satellite Analysis Branch. Other IR-based automated methods have been developed (Ritchie et al., 2012; Kishimoto et al., 2013; Zhao et al., 2016), and most recently artificial intelligence-based Machine Learning (ML) approaches are emerging. For example, early studies by Chen et al., (2019), Lee et al., (2020), Zhuo and Tan, (2021) and Higa et al., (2021) demonstrated the promise of applying Machine Learning (ML) to train on large IR datasets and skillfully estimate TC intensity. Olander et al., (2021) examined the potential to employ ML enhancements to the ADT. It was found that ML could augment the ADT by interrogating features that are output from the ADT image processing, resulting in significant improvements in the accuracy of TC intensity estimates over the ADT itself. This algorithm (AiDT) is now operational at NOAA/NESDIS. More recently, a Convolutional Neural Network model coined D-PRINT (DeeP learning IR INtensity of TCs) was developed to operate and train on a large sample of TC-centered IR images. As reported in Griffin et al., (2024), this method shows comparative skill to the ADT/AiDT in some TC basins and improvement in others. Real-time D-PRINT estimates for global TCs can be found on the CIMSS TC web site listed in Appendix A.

2.3. Atmospheric motion vectors

Geostationary satellites also provide multispectral imagery for tracking clouds and water vapor motions over the global tropics. Quantifying these motions into atmospheric motion vectors (AMVs) provides crucial information on near-environment flow regimes that dictate TC steering. Multiple satellite agencies are now deriving these AMVs over tropical regions using fully automated algorithms with greater spatiotemporal coverage and height assignment precision than ever before. Operational GOES AMVs produced by NOAA/NESDIS have been shown to positively impact hurricane model forecasts (Lim et al., 2022). Nonaka et al., (2016) developed a sea-surface wind product from adjusted low-level Himawari AMVs, coined ASWind, by training with coincident sea-surface winds retrieved by ASCAT. The product can be useful for estimating TC outer surface wind radii.

Recent research efforts have focused on novel methods to extract high spatiotemporal vortex-scale AMV fields from rapid-scan sectors that follow targeted TCs. For example, Stettner et al., (2019) employs traditional and optical flow cloud tracking methodologies along with TC-focused processing strategies to derive ultra-high density AMV fields using GOES 1-min. interval meso-sector scans. This product focuses on the storm-top central dense overcast (CDO). Figure 5 shows an example of datasets processed in real time by CIMSS during Hurricane Beryl (2024). The assimilation of these specially processed AMV datasets into high-resolution TC models has produced positive impacts on forecast track and intensity (Velden et al., 2017; Li et al., 2020). The resulting cloud-top motion fields can also be used to assess outflow configurations/changes, vertical wind shear, divergence, and radial imbalances that can signify short-term intensity changes (Velden and Stettner, 2018; Ryglicki et al., 2019, 2021; Knaff, 2024). The TC-focused GOES AMV product is in operational transition at NOAA/NESDIS.

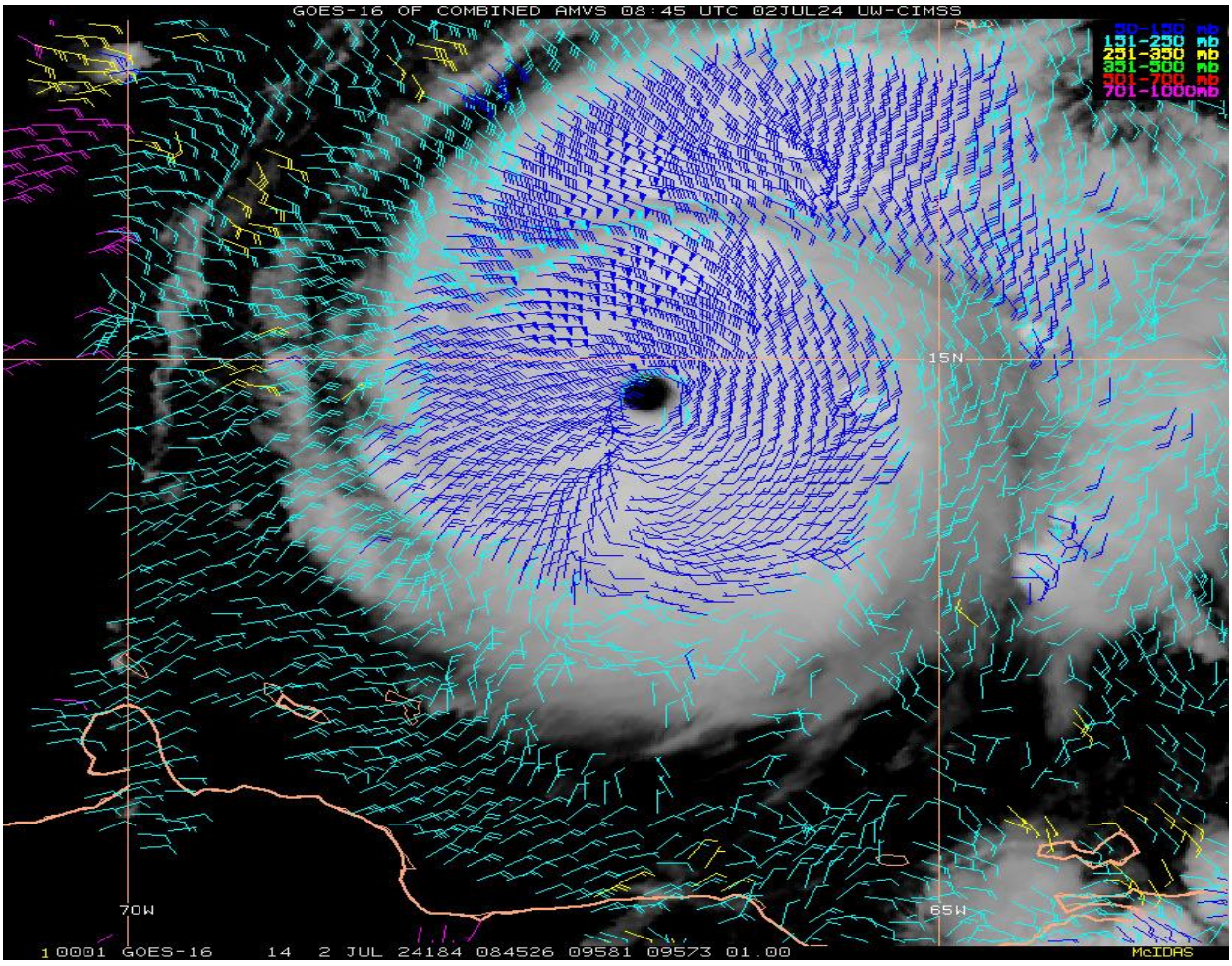

Fig. 5. GOES-East meso-sector scan ultra-high-density AMVs derived from 1-min. interval meso-sector scans during Hurricane Beryl (2024). Plotted vectors are thinned for presentation and color-coded by assigned heights (hPa) shown in the upper-right (hPa). [Source: CIMSS]

Animated sequence:
https://tropic.ssec.wisc.edu/real-time/mesoamv/2024/02L/plots/temp/Beryl.gif (animation of Fig. 5 for the period 29 June – 5 July 2024 shown at 15-min. intervals)

Tsukada and Horinouchi, (2020), Tsujino et al., (2021), Horinouchi et al., (2023) and Tsukada et al., (2024) demonstrate that special Himawari-8 rapid-scan operations observing TCs at 2.5-min. or even 30-sec. imaging intervals can effectively reveal transient asymmetric disturbances within the TC inner-core region and allow for estimates of low-level tangential winds inside clear TC eyes. Figure 6 illustrates an example of this capability using the approach from Tsukada et al., (2024). The AMVs quantify the asymmetric motions seen moving around the eye due to transient wavenumber-1 features (mesoscale vortices, Nolan and Montgomery, 2000) which can contribute to the inward transport of angular momentum and acceleration of eye rotation. Although relatively few TCs have large clear eyes, the capability to estimate wind speeds in the inner-core region of intense TCs suggests the potential for improved vortex initialization and/or data assimilation in TC forecast models. Automation of the method application and research on data assimilation impact is underway.

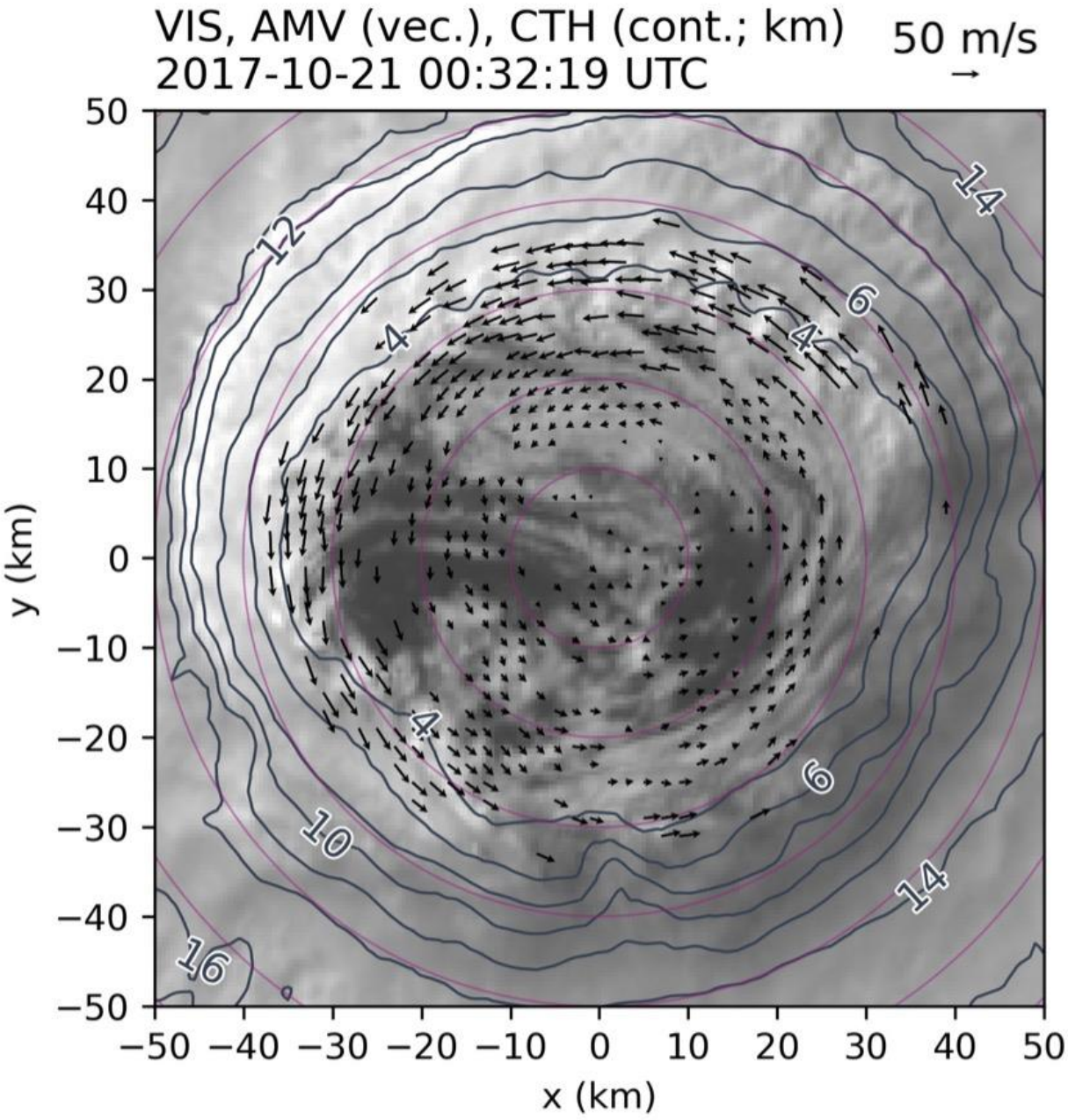

Fig. 6. An example of AMVs in the eye of Typhoon Lan (2017) obtained from a Himawari satellite 2.5-min interval VIS image sequence. The AMVs (black vectors) overlay the storm-centered VIS image at 0032 UTC on 21 October 2017, with the vector length corresponding to cloud motion speed. The contours represent cloud-top heights (km) obtained from 10.4-μm IR Tb and ERA5 re-analyses. [From Tsukada et al., 2024]

Animated sequence:
https://drive.google.com/file/d/1c_BWu-ejEn2Ia8K3MEZz6vQjvJuWCfNI/view?usp=sharing

3. TC applications from LEO passive microwave sensors

Satellite-based passive microwave (PMW) radiometers are "keystone" sensors for monitoring TCs due to their ability to view critical structural features that otherwise can hide under the central dense overcast as viewed by VIS/IR sensors. PMW imagers carry a suite of channels that enable the retrieval of surface wind speeds over oceans, rainfall rate, total precipitable water (TPW) and cloud liquid water among other parameters. PMW sounders are capable of sensing tropospheric temperature profiles in the TC core for intensity estimation and phase analysis. Presented below are some examples of applications to TCs.

3.1. Novel uses of PMW imagers

Operational TC warning centers around the globe have increasingly utilized PMW imager information since they first became available with the U.S. Defense Meteorological Satellite Program (DMSP) Special Sensor Microwave Imager (SSM/I) in 1987. This sequence of sensors was then followed by a combination of operational and research mission instruments (TMI, WindSat, SSMIS, MWRI, AMSR2, GMI). The longevity of these sensors has significantly improved TC temporal sampling (Hawkins, et. al., 2025). While the SSMIS sensors are ageing off, the next generation of PMW imagers are emerging as part of the U.S. DoD Weather System Follow-on – Microwave (WSF-M) satellite program (WMO, 2024a), the JAXA GOSAT-GW (AMSR-3), and the Chinese FY-3 series. The first of two scheduled rainfall missions, FY-3G, successfully launched in 2023, carries both a passive microwave radiometer and an active precipitation measuring radar (Zhang et al., 2023).

For TC analysis, the PMW imagers with Ku-band (30-49 GHz) and W-band (85-92 GHz) channels have performed well for surveilling TC rainbands and eyewalls (Hawkins and Velden, 2011). Rain and frozen hydrometeors have an impact on brightness temperatures (Tb) in these bands, thus making them valuable contributors for monitoring TC convective structural changes. As illustrated in Fig. 7, visible and IR imagers often can't observe key TC features hidden under the central dense cloud overcast such as low-level circulation centers (Fig. 7a), organization of convective structure related to TC intensity (Fig. 7b), and eyewall events (concentric eyewalls, eyewall replacement cycles, Fig. 7c). The corresponding PMW products in these examples are color-enhanced with channel compositing and breakpoints specifically designed for TC applications (Hawkins et al., 2004).

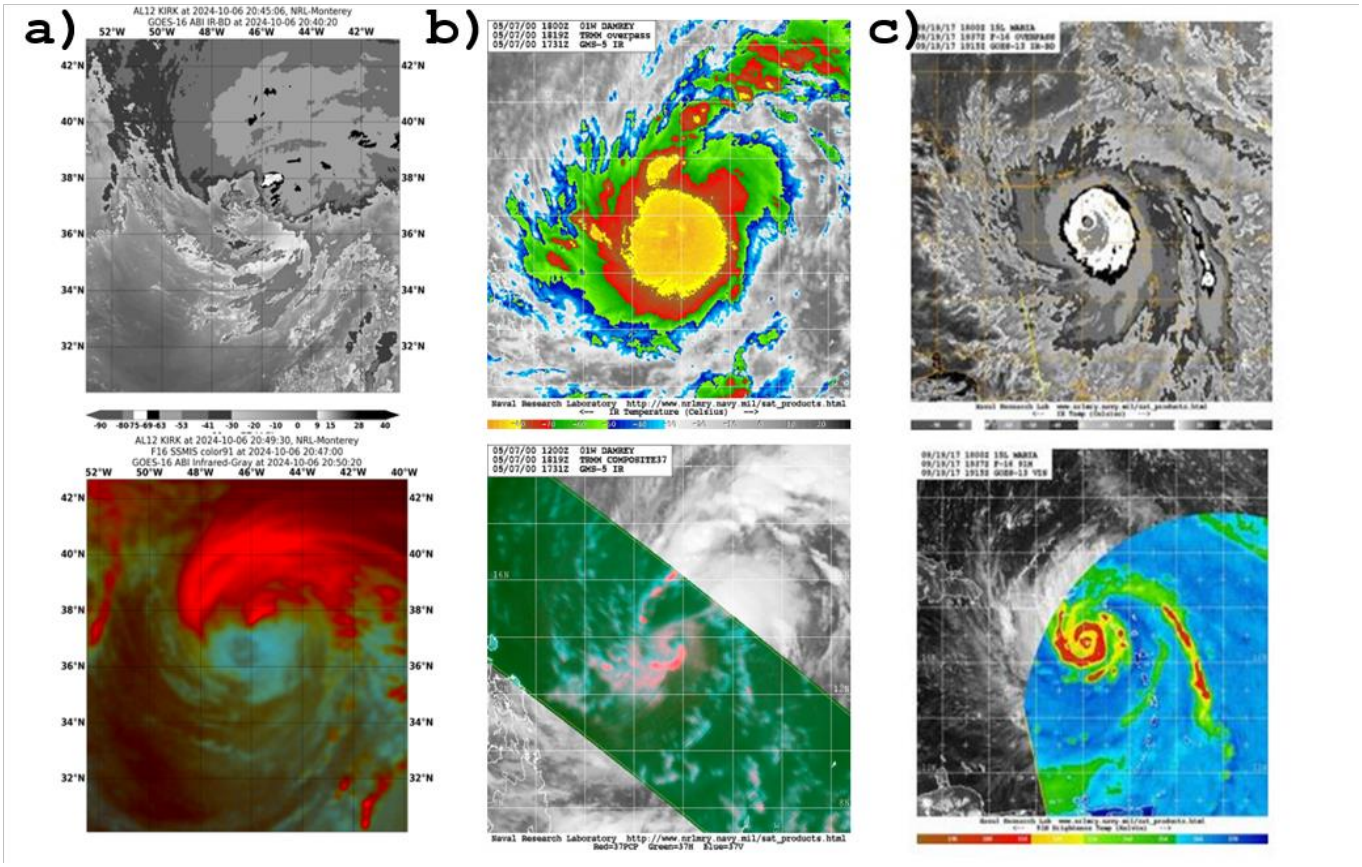

Fig. 7: Examples of PMW imagery aiding the analysis of TCs. a) Tropical Storm Kirk at 2045 UTC on 6 Oct. 2024: enhanced GOES-16 IR (top) and the coincident SSMIS 92 GHz color product below. b) Typhoon Damrey at 18 UTC on 7 May 2000: color-enhanced GMS-5 IR (top) and the coincident TRMM 37 GHz color product below. c) Hurricane Maria at 18 UTC 19 Sept. 2017: GOES-13 enhanced IR (top) and the coincident SSMIS 92 GHz H-pol image below. [Images courtesy NRL-MRY web site]

3.2. PMW ocean surface wind speeds from L-band radiometers

Two research satellites house L-band radiometers (sensing between 1 and 2 GHz) and provide ocean surface wind speed estimates; the NASA Soil Moisture Active Passive (SMAP; Entekhabi et al., 2010, 2014) and the ESA Soil Moisture Ocean Salinity (SMOS; Kerr et al., 2010; Mecklenburg et al., 2016). The passive SMAP radiometer uses a 6-m physical dish, whereas SMOS uses a synthetic aperture resulting in modest spatial resolutions of ~ 40 km. However, with diminished precipitation attenuation effects, these instruments can effectively sense strong to extreme TC wind speeds from 15 to 75 ms^{-1} (Meissner et al. 2017; Reul et al. 2017) but require ancillary SST and ocean salinity estimates to do so. They are among the few instruments that can provide reasonable estimates of 34-kt wind radii in the majority of TCs and even 50- and 64-kt wind radii for most average and large-sized TCs (Knaff et al., 2021). Remote Sensing Systems (REMSS) provides SMAP and ESA SMOS wind speed images in near real-time for use by TC forecast centers.

Sensors with C and X bands (WindSat, AMSR-E, AMSR2) have also provided ocean surface winds for TC applications. The AMSR2 algorithms were updated using the full suite of channels (6-89 GHz) trained with coincident SMAP values to remove spurious artifacts due to high rain attenuation, and then validated (Meissner, et. al., 2021; Manaster et al., 2021). The AMSR2 TC wind speed product can be considered on par with SMAP, although some residual attenuation artifacts are possible with intense rain rates and winds below hurricane-force (Ricciardulli et al., 2023). This advancement provides optimism for accurate retrievals from AMSR3 which is scheduled to launch in 2025. Gridded AMSR2 maps and fixes are available in near real-time on the REMSS web site (example shown in Fig. 8), and global all-weather AMSR2 winds are produced by NOAA (Alsweiss et al., 2021) and by JAXA (Shibata, 2006).

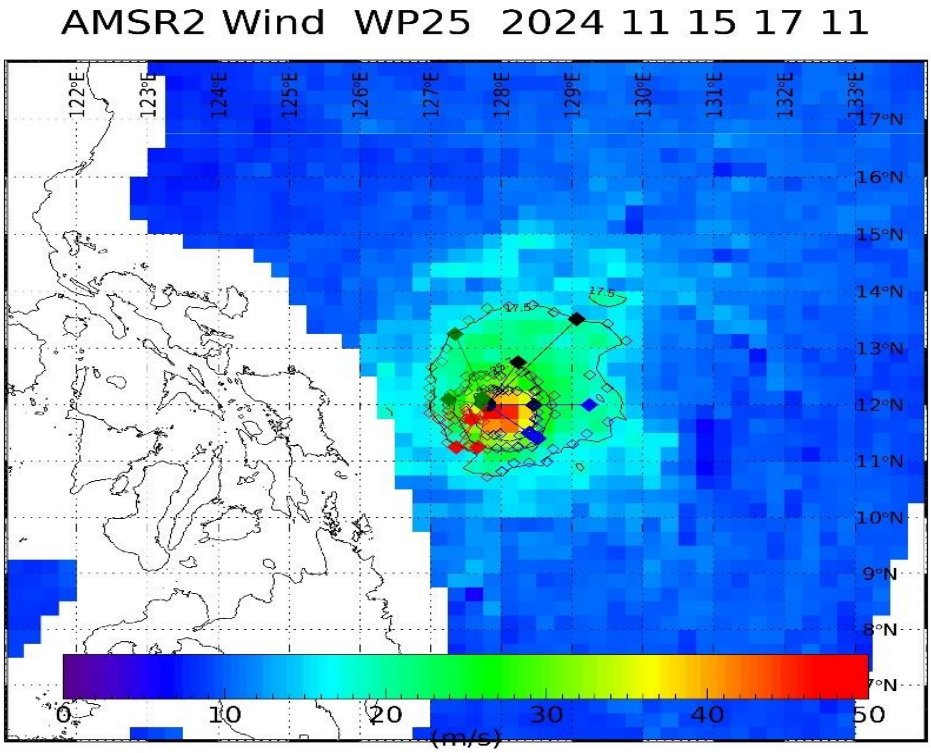

Fig. 8. AMSR-2 surface wind speeds (ms^{-1} via the color table) for Typhoon Man-Yi at 1711 UTC on 15 Nov. 2024. Plotted diamonds represent extent of critical wind radii from Man-Yi's center, color coded by storm-relative quadrant. [Credit: REMSS]

3.3. PMW sounder-based TC intensity estimates

A signature characteristic of TCs is the development of a mid-to-upper tropospheric warm core as the cyclone organizes and intensifies. LEO PMW sounders are capable of sensing tropospheric temperature structures at altitudes determined by the weighting function for each channel using the oxygen band in the ~55 GHz range. Several TC intensity estimation algorithms have been developed based on the strength of the warm core and hydrostatic principles, leveraging either PMW sounder Tb or temperature retrievals (Brueske and Velden, 2003; Demuth et al., 2006;

Bessho et al., 2010; Oyama, 2014). Zhang et al., (2019) extended the concept to the 118 GHz channels of the Microwave Humidity and Temperature Sounder (MWHTS) onboard the Chinese FY-3C satellite and achieved similar good estimates of TC surface pressure anomalies. While initial intensity estimation methods focused on estimating the TC MSLP due to the more direct relationship between the observed thermal anomaly and the surface pressure perturbation, most algorithms now also estimate the maximum sustained surface winds.

Special Sensor Microwave/Sounder (SSMIS) instruments became available in late 2005 aboard the U.S. DoD DMSP satellites (Hawkins et al., 2025). Since then, the NASA Advanced Temperature Microwave Sounder (ATMS) launched in 2012 aboard Suomi-NPP and the follow-on NOAA Joint Polar Satellite System (JPSS) missions with their improved spatial resolution have resulted in better views of the TC warm core (Fig. 9) and improved TC intensity estimation skill. Unfortunately, the DMSP sounders are well past their expected lifetime and now provide very limited data. However very recently, innovations in satellite design and launch capabilities have permitted much smaller microwave sounders in the form of LEO Smallsats and CubeSats. One such example is the NASA TROPICS mission (Blackwell et al., 2018), starting with the Pathfinder satellite in 2021 and the constellation completed in 2023 with four additional CubeSats sensing the 92, 118, 183 and 205 GHz frequencies. This proof-of-concept mission has been successful in demonstrating lower-cost alternatives for frequent LEO PMW sampling of TCs.

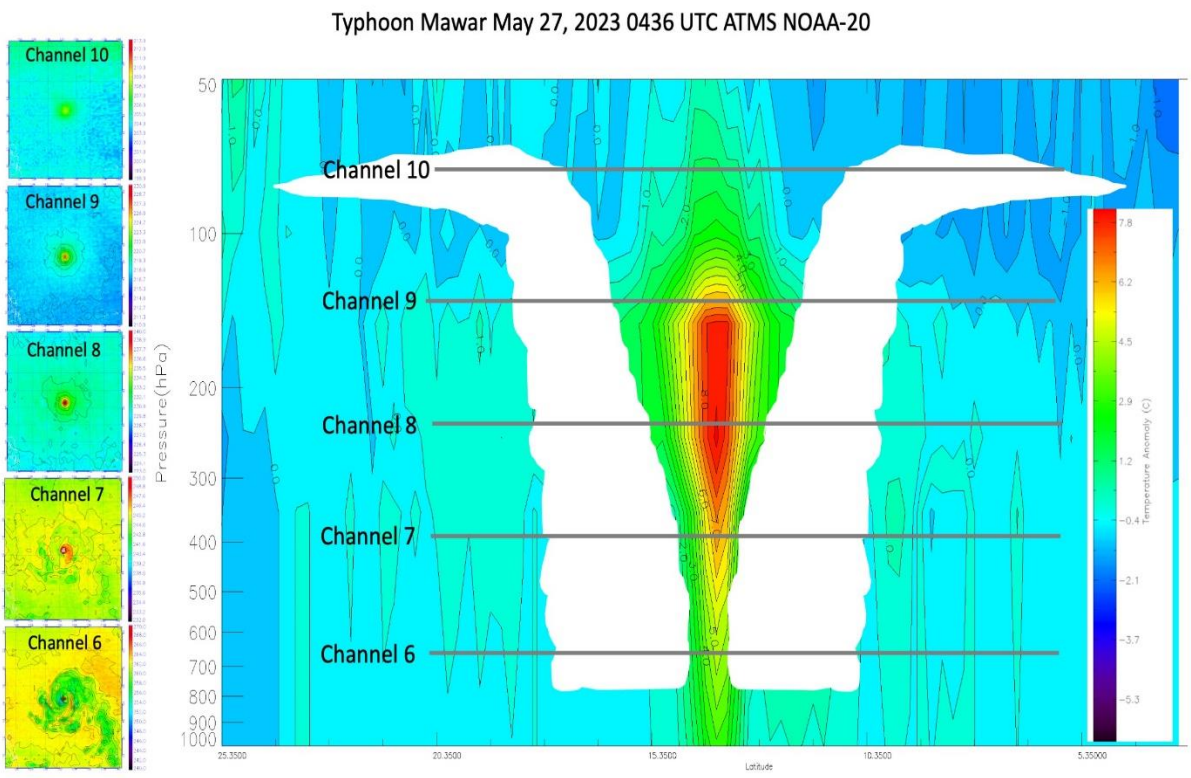

Fig. 9. View of Super Typhoon Mawar from a NOAA-20 ATMS overpass at 0436 UTC on 27 May 2023. Planar Tb views from the sounder thermal channels 6-10 shown on the left coincide with their approximate altitudes shown in the longitudinal cross-section of Tb thermal anomaly (deg. C) through the center of Mawar. The TC warm core is evident as red. Eyewall clouds (white) drawn on the cross-section are for effect. [Fig. prepared by CIMSS]

Recent advancements in ML techniques such as Convolutional Neural Networks (CNNs) have also allowed for the estimation of TC intensity from the sounder moisture channels in the 183 GHz range (which is available on many LEO satellite radiometers). These ML techniques rely on TC precipitation structure and organization, and in many cases show superior skill to the temperature-based methods (Griffin et al., 2024). Future work to exploit both the temperature and moisture channels together using these methods may advance the skill further.

3.4. Other TC-focused PMW-based products

An eyewall replacement cycle (ERC) process is known to have a disruptive impact on the TC inner core that often results in a period of weakening. However, the TC central dense overcast often masks ERC events in IR imagery, resulting in intensity forecast errors. PMW imagery is particularly useful for identifying ERCs. Sitkowski et al., (2011) looked at the evolution of the TC inner wind field reorganization during ERC events using aircraft data and documented the changes with respect to the presentation in PMW 85-92 GHz imagery. Kossin et al., (2023) expanded upon these findings to develop an algorithm called the Microwave Probability of Eyewall Replacement Cycle (M-PERC) to predict the onset of ERCs. The technique relies on "Ring Scores" from the ARCHER algorithm (Section 5) that measures the fit of the gradients of Tb in the PMW imagery to a circular shape. Figure 10 is an example output from M-PERC for TC Darian (2022) showing a Hovmöller plot of PMW ring scores and the development of an outer ring (secondary eyewall formation, or SEF, which is often the start of an ERC). Note the corresponding increase in model ERC probabilities rising to near 70% for the full model that uses the PMW score predictors. Shortly thereafter, the analyzed TC intensity shows a subsequent leveling off and decline.

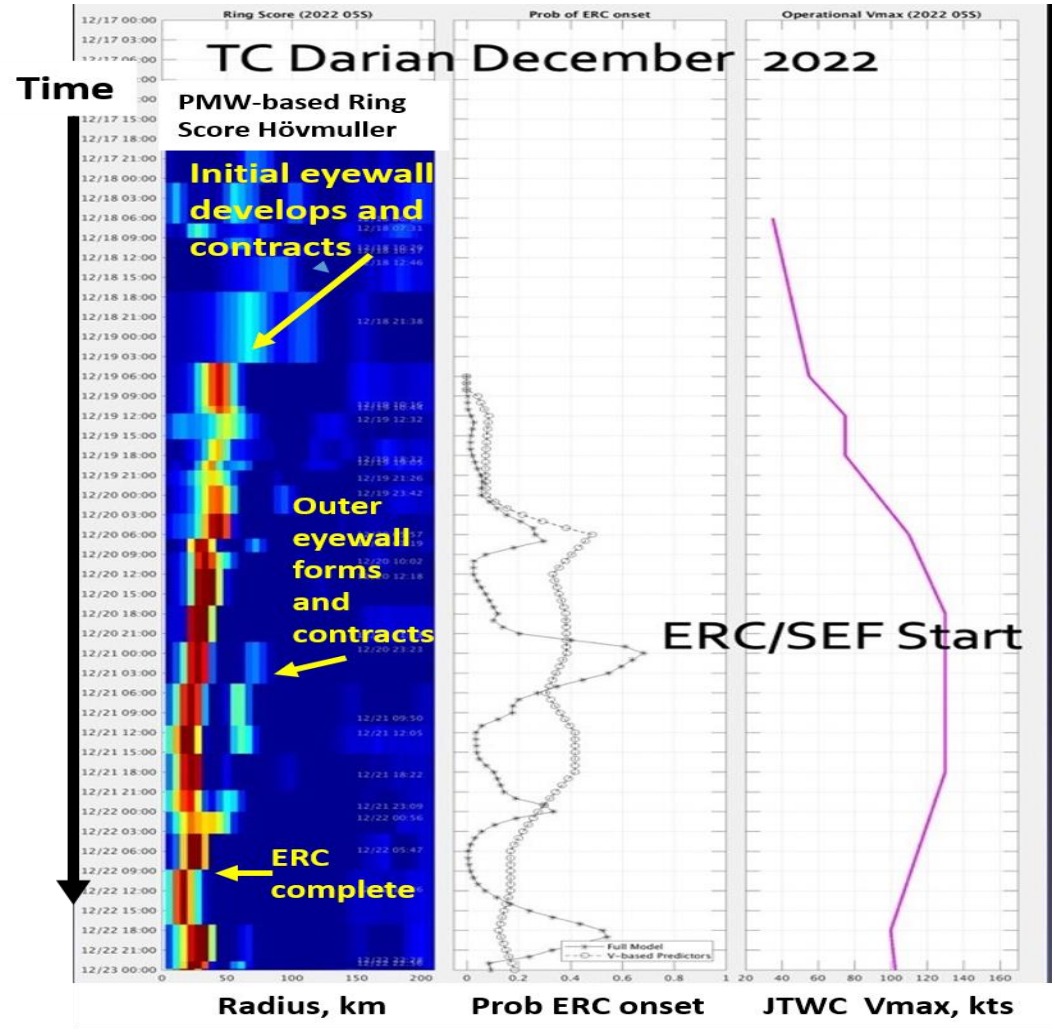

Fig. 10. M-PERC algorithm display for TC Darian 17-22 Dec. 2022. Left: Hovmöller plot of PMW ring scores vs. radius from TC center (warmer colors > stronger eyewall signature). Middle: the probability output from two logistic regression models (simple V-based, and Full with PMW info). Right: JTWC working Best Track intensities (Vmax). Full model peak in probability of Secondary Eyewall Formation (SEF) signals the start of an ERC process and period of arrested intensity of Darian. [Credit: CIMSS]

Additional tools utilizing multiple PMW satellites that can be applied to TC analysis include the Integrated Multi-satellitE Retrievals for GPM (IMERG) algorithm (Huffman et al., 2015) and the Climate Prediction Center MORPHing technique (CMORPH, Joyce et al., 2004). Wu et al., (2024) presents a recent assessment of these products for TC cases off the east coast of China. Two other integrated PMW products for monitoring TC evolution are based on the Morphed Integrated Microwave Imagery at CIMSS (MIMIC) methodology: For TC structural evolution, MIMIC-TC (Wimmers and Velden, 2007), and for monitoring TC moisture environments such as Total Precipitable Water, MIMIC-TPW (Wimmers and Velden, 2011). These products merge PMW data into seamless animations that display a continuous real-time hourly-interpolated evolution of the TC and its environment (both products available on the CIMSS TC site, see Appendix A for link).

4. TC applications from active transmission systems

4.1. Scatterometers

Scatterometers are LEO-based active remote sensing instruments that transmit microwave pulses towards the Earth's ocean surface and measure the backscattered signal to gather information. They are typically used to determine ocean surface vector winds (OSVW) by analyzing the scattering from small-scale waves on the surface. Scatterometers have a three-decade legacy for providing extremely valuable data for TC applications, and more missions are becoming available. Specifically for TC surveillance, the data are critical for determining if a disturbance has a closed surface circulation, the areal extent of that TC circulation (i.e. TC size), and for estimating outer vortex critical wind radii (commonly used wind thresholds by many operational TC forecast centers to communicate the extent of potentially impactful TC winds, and for vortex initialization input to TC models).

Currently, C-band (e.g., European MetOp ASCAT) and Ku-band (e.g., Indian OceanSat-3 OSCAT; Chinese HY2 HSCAT) scatterometers are operational (about a half-dozen total) and provide OSVW swaths of ~1100-1800 km in width with ~12.5 to 50 km spatial sampling. While the past legacy of scatterometers monitoring TCs was often 'hit or miss', the current era of multiple satellite agencies operating scatterometers is providing unprecedented temporal sampling of TCs (e.g., EUMETSAT, 2021). In the near future, a concerted effort by EUMETSAT, CMA, NSOAS, and ISRO will typically provide a scatterometer hit of a TC every few hours (WMO, 2025). This aspect is particularly important for real-time TC analysis, especially TCs undergoing rapid surface wind field evolution. The higher sampling should also benefit TC research studies. For example, Fig. 11 illustrates OSVW fields from two ASCAT overpasses just 50 minutes apart during the formative stage of Typhoon Nyatoh in 2021. The zoomed-in boxes over the same area show changing surface convergence and divergence likely due to moist convective processes (King et al., 2022). No other observing system can detect such changes at these spatiotemporal scales. Since moist convection processes drive TCs, such information could contribute to further understanding and modeling of the relationship between dynamical moist convection processes and TC evolution.

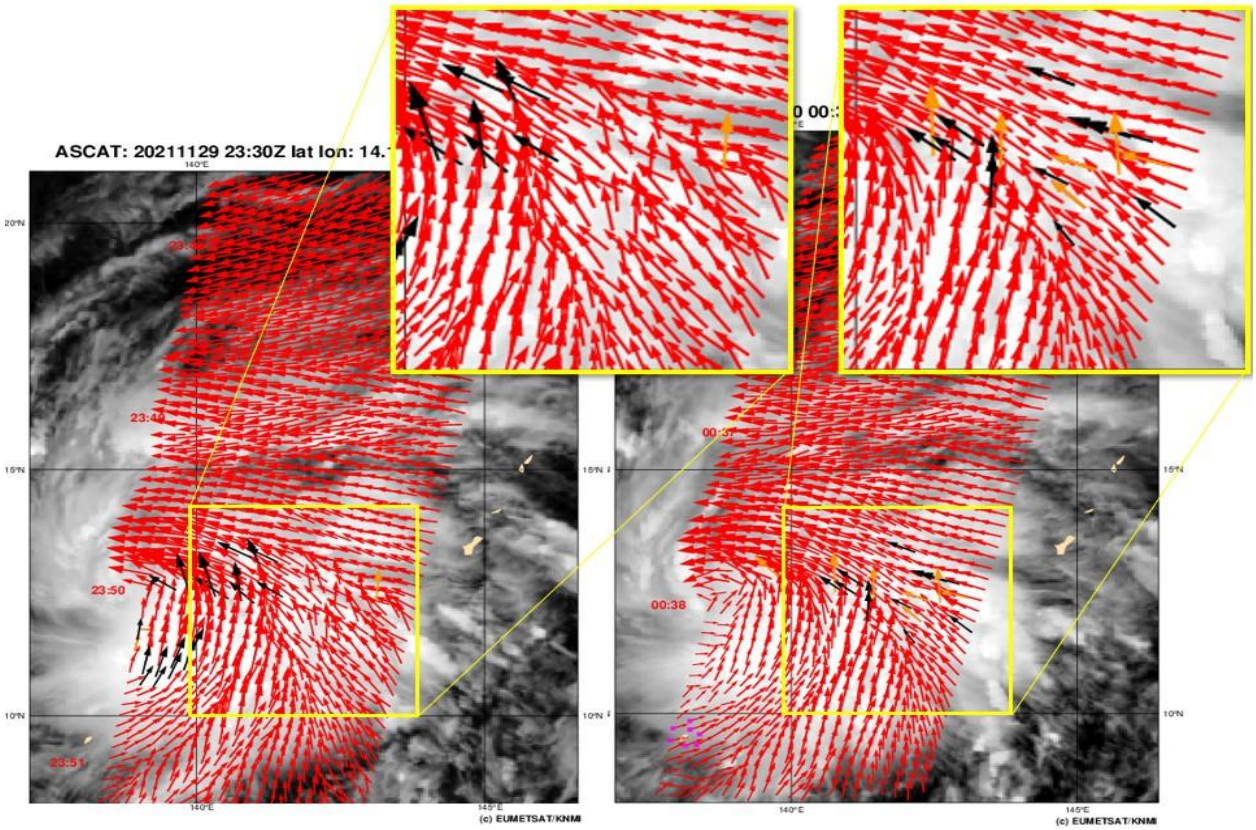

Fig. 11. ASCAT-C overpass of TC Nyatoh on 29 Nov. 2021 at 23:30 UTC (left) and 60 minutes later by ASCAT-B (right) depicting OSVW plotted over concurrent Himawari IR images. The zoomed images of the same area show the short-term changes in the surface wind field. Black and orange vectors are QC-flagged data. [Credit: EUMETSAT OSI SAF/KNMI]

The moderate spatial resolution of the scatterometer OSVW products has traditionally resulted in relatively low estimates of higher TC wind speeds (above 20 ms^{-1}), whereas recent studies show that adjusted scatterometer winds are capable of estimating these stronger winds (Polverari et al., 2022; Ni et al., 2022). However, it should be noted that it is difficult to directly compare various operationally available TC wind speed products as they have not been consistently calibrated (Stoffelen et al., 2021). KNMI, NOAA/NESDIS and REMSS process all ASCAT data into OSVW with slightly different algorithms and calibrations (Stoffelen et al., 2020; Soisuvarn et al., 2013: Ricciardulli and Manaster, 2021). KNMI also operationally processes other scatterometer data from NSOAS/CMA (China) and ISRO (India). NSOAS currently processes data from the FY-2A scatterometers (HSCAT-B, -C and-D) (Wang et al., 2020; 2021; Yang et al., 2023). The CMA also launched a novel dual-frequency (C- and Ku-bands) rotating fan-beam scatterometer (Li et al., 2018) called WindRad in 2021 on FY-3E. Finally, the recently launched ISRO OceanSat-3 OSCAT is now producing operational products available through ISRO, KNMI and NESDIS. See Appendix A for some of the links to current scatterometer products and distribution. In the coming years, Europe, China and India will launch further scatterometers for operational use. For example, in 2026 EUMETSAT will launch the first MetOp-SG-B series scatterometer (SCA), a next generation of C-band ASCAT with VH/HV cross polarization and improved spatial resolution (Rostan et al., 2016) that will further aid the detection of higher TC wind speeds, with plans to launch two more SCAs through 2045.

In summary, there are many current and planned scatterometers designed to supply high-quality OSVW that can capture TC surface wind field evolution. Recent innovations in wind speed calibration and adjustment methods employed for scatterometers can be extended to SARs and other microwave sensing of TC wind speeds (Portabella et al., 2022). Progress in OSVW retrieval accuracy at higher wind speeds owing to e.g., SAR comparisons (thanks in large part to ESA's Satellite Hurricane Observation Campaign (SHOC)) has improved both scatterometers and SARs as complementary satellite-based tools for TC monitoring. Moreover, image resolution enhancement and SAR-trained structure function methods (Alsweiss et al., 2024; Ni et al., 2024) show promise in augmenting the observations by scatterometers to better capture higher-resolution TC wind field features. Future scatterometer missions will explore enhanced wind speed sensitivity in TCs by using cross-polarized microwave backscatter techniques.

4.2. Synthetic Aperture Radar (SAR)

The utilization of SAR data for TC analysis began in earnest with ESA's Sentinel-1 satellite in 2014, prompted by three factors: 1) Sentinel-1 data was freely available, 2) the establishment of a dedicated field experiment (SHOC) to collect data over TCs with the support of ESA, and 3) methods were developed to combine the co- and cross-polarized signals to estimate extreme wind speeds (Mouche et al., 2017, 2019). Since that time, and with appreciation to the Canadian Space Agency (CSA), three additional satellites from the RadarSat Constellation Mission (RCM) are now routinely scheduled to target TCs. Figure 12 illustrates the coverage achieved by the constellation of C-band SAR passes during Tropical Cyclone Anggrek (2024). Other existing SAR missions such as ALOS-2 L-band SAR from JAXA or EOS-4 C-band SAR from ISRO could join this constellation. The ALOS-2/ Phased Array L-band Synthetic Aperture Radar-2 (PALSAR-2) has already observed TCs, demonstrating encouraging results (Isoguhi et al., 2021). Emergent SAR satellite capabilities include JAXA's ALOS-4/PALSAR-3 mission (launched in 2024), the NASA-ISRO SAR (NISAR) mission (expected launch in 2025), and the Sentinel-1C and -1D (launches in 2024/2025) with identical capabilities as Sentinel-1A and -1B. These new additions hold promise for improving TC extreme surface wind speed estimates if and when targeted TC acquisitions can be scheduled (current SAR instruments cannot provide orbit-wide coverage due to power constraints).

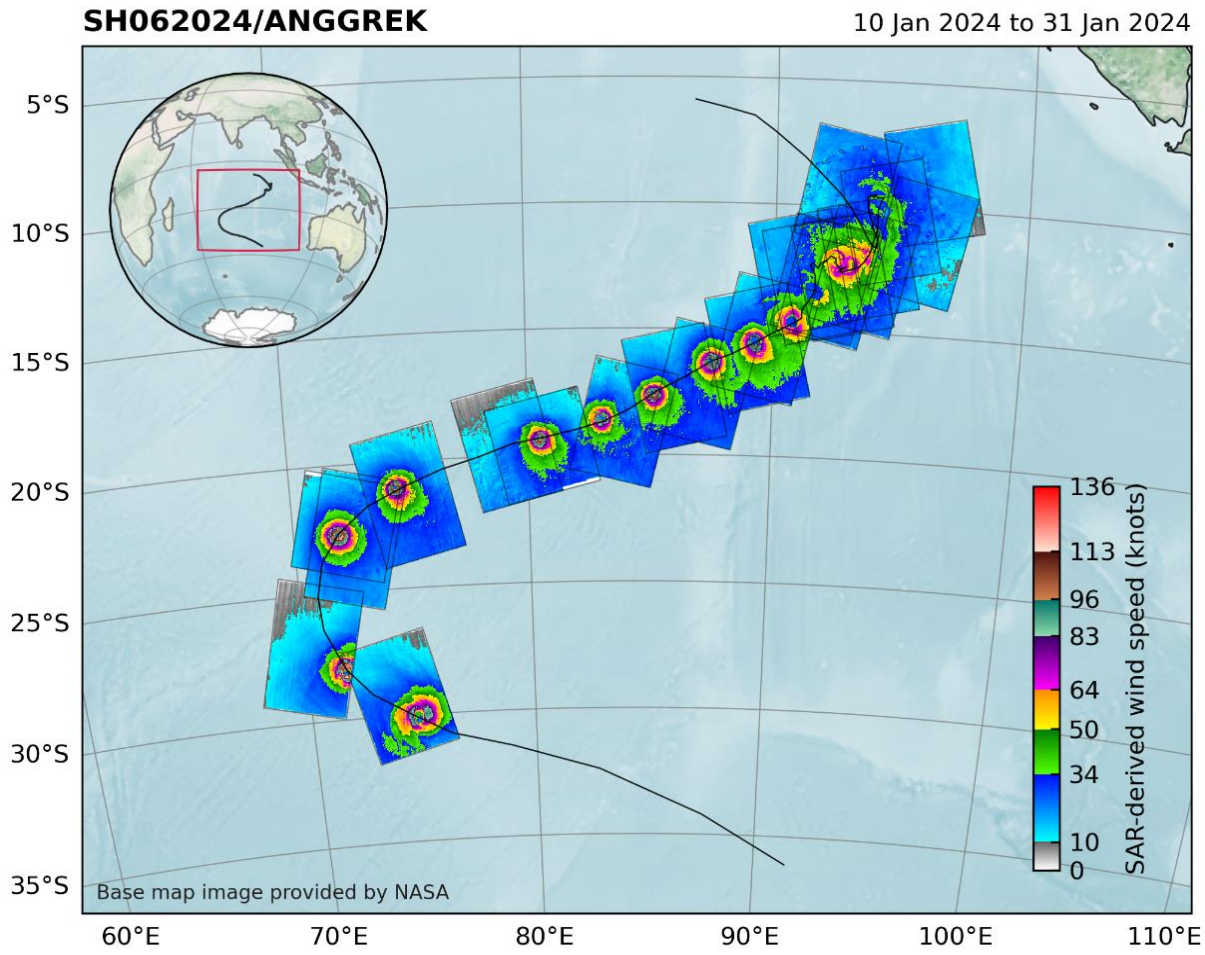

Fig. 12. Coverage achieved by the constellation of C-band SAR passes during Tropical Cyclone Anggrek passage over the south Indian Ocean in Jan. 2024. [Fig. prepared by CIRA]

The SAR and TC communities (IFREMER, NOAA/STAR, and NRL-MRY) work together to make near real-time TC surface wind fields from Sentinel-1A/B, RadarSat-2, and RCM available to both TC research and operational communities worldwide. Estimates of maximum sustained 1-min. surface winds, radius of maximum wind, and critical wind radii in storm-relative quadrants are now available and consolidated based on inputs from both communities (Jackson et al., 2021; Howell et al., 2022). Efforts continue to address improvements to the wind retrieval algorithm, quality control, and dynamic averaging strategies addressing the known shortcomings associated with cloud ice scattering (e.g. Alpers et al., 2021; Subrahmanyam et al., 2023) and rain attenuation (e.g. Mouche et al., 2019). The high spatial resolution of the observations make SAR an ideal platform for examining TC inner-core surface wind structure, especially for estimating the storm center and the radius of maximum winds (Combot et al., 2020a; Tsukada & Horinouchi, 2023). Furthermore, many research topics rely on SAR observations including TC dynamics (e.g., Avenas et al., 2023, 2024; Huang et al., 2018; Vinour et al., 2021), ocean response to TCs (Combot et al., 2020b), TC surface structure analyses (Shimada et al., 2024; Moore Torres et al., 2023), effects of rainfall on wind speed estimates (Guo et al., 2022) and TC data assimilation (Ikuta and Shimada, 2024).

4.3. Doppler Wind Lidar

The Aeolus satellite carries a Doppler Wind Lidar (DWL) instrument launched by ESA in 2018 that can provide global tropospheric wind profiles with high vertical resolution in clear air and also winds at cloud tops. The primary instrument, called ALADIN, actively transmits laser pulses and measures the backscattered light to determine wind speeds at different atmospheric levels (Straume et al., 2020). Assimilating the horizontal line-of-sight wind data along the satellite's path (mainly the zonal component in tropical latitudes) has generally had positive impacts on NWP. While the DWL cannot provide vertical wind profiles under the dense TC overcast, vertical wind profiles in the adjacent cloud-free environment can help define steering flows and TC-environment interactions. Impacts of the assimilated data on TC track and intensity forecasts in TC models have been modestly positive (Garrett et al., 2022; Marinescu et al., 2022; Okabe and Okamoto, 2024).

4.4. Radar altimetry

Satellites have long contributed to sea surface temperature (SST) analyses. To first order, the SSTs beneath the eyewall of TCs determine the maximum potential intensity (Emanuel, 1988; Miller 1958). However, the integrated energy of the ocean determined from the depth of the 26ºC isotherm, or Ocean Heat Content (OHC), can perhaps be a better determinant of the energy reservoir available to the TC, and an important influence on TC intensity. Knowledge of the OHC and SST in the path of an approaching TC can improve the short-term forecast of its intensity (Goni et al., 2009, and references within). Satellite altimetry was first demonstrated by the U.S Navy GEOSAT missions in the 1980s, followed by the joint NASA and French TOPEX/Poseidon which provided the basis for the first methods to estimate OHC (Goni et al., 1996; Shay et al., 2000). While these methods still exist making use of TOPEX and JASON-1,-2,-3 satellites, today OHC typically relies on global ocean model analyses (e.g., Sampson et al., 2022) where synthetic soundings based on satellite altimetry are assimilated along with other in situ ocean soundings. The current primary source for altimetry data is the Sentinel-6 Michael Freilich satellite, often referred to as marking a "golden age" of satellite altimetry due to its high precision measurements.

4.5. GNSS radio occultation

Atmospheric soundings are now possible using a technique called Global Navigation Satellite System Radio Occultation (GNSS-RO) which measures the bending of L-Band radio waves as they pass through the atmosphere. GNSS-RO leverages signals from GPS satellites to measure atmospheric conditions, providing high vertical resolution data without relying directly on microwave radiation like traditional PMW sensors do. The unique properties of GNSS-RO include global 3-D coverage (40 km to the surface), good vertical resolution with all-weather precise temperature sounding accuracy, and assured long-term stability of observations. Currently, the Constellation Observing System for Meteorology Ionosphere and Climate-2 (COSMIC-2) RO satellite constellation is providing data that has shown promise to improve TC intensity forecasts when assimilated into a hurricane model (Miller et al., 2023).

4.6. GNSS reflectometry

A LEO satellite constellation launched in 2016 to demonstrate a novel approach for retrieving surface winds in TCs is the NASA CYclone Global Navigation Satellite System (CYGNSS) mission (Ruf et al., 2018). With inclined orbits to focus coverage over the tropics, CYGNSS employs the GNSS and L-band reflectometry to measure oceanic surface winds. Ruf et al., (2019)

provides an initial assessment of retrieved wind speed quality, with the algorithms since corrected for various biases. Ricciardulli et al., (2021) provides an assessment of different CYGNSS wind products in TCs. Research-quality datasets are being produced by the University of Michigan (Ruf et al., 2019) and NOAA/NESDIS/STAR (Said et al., 2021), and these are available on the NASA JPL Distributed Active Archive Center. Another GNSS venture recently launched by China provides two different GNSS reflectivity wind products from the GNOS-II payload on the FengYun-3E (FY-3E) satellite: A global wind product optimized for low-to-medium ocean surface wind speeds, and a cyclone wind product optimized for high wind speeds in tropical and extratropical cyclones (Huang et al., 2022). Sun et al., (2023) evaluated the cyclone product in TC conditions and found an accuracy of 3-3.5 ms^{-1} however with few validation cases above 45 ms^{-1}.

5. TC applications from blended satellite products

In addition to 'stand-alone' products or algorithms, novel ways of integrating satellite-derived data by blending attributes from multiple sources can aid in TC analysis and forecasting. For example, NOAA/NESDIS maintains many operational satellite products that include blended global SSTs (Maturi et al., 2017), the Multi-platform Tropical Cyclone Surface Wind Analysis (MTCSWA; Knaff et al., 2011), the Tropical Cyclone Formation Product (TCFP; NOAA/NESDIS, 2024), blended Total Precipitable Water (bTPW; Kidder and Jones, 2007), the Advective Layered Precipitable Water (ALPW; Forsythe et al., 2015), the ensemble Tropical Rainfall Potential (eTRAP; Ebert et al., 2011) and the Hurricane Intensity and Structure Algorithm (HISA; NOAA/NESDIS, 2024). Data from multiple LEO microwave sounders provide important inputs to eTRAP, MTCSWA, bTPW, ALPW and HISA, the latter four via the Microwave Integrated Retrieval System (MIRS, Liu et al., 2020). MTCSWA and TCFP make use of global GEO data. The operational version of MTCSWA uses ASCAT and low-level AMVs, while the developmental version also makes use of SMAP, SMOS, and AMSR2 wind speeds (RAMMB, Appendix A). Figure 13 presents an example of the MTCSWA product for Typhoon Usagi (2024).

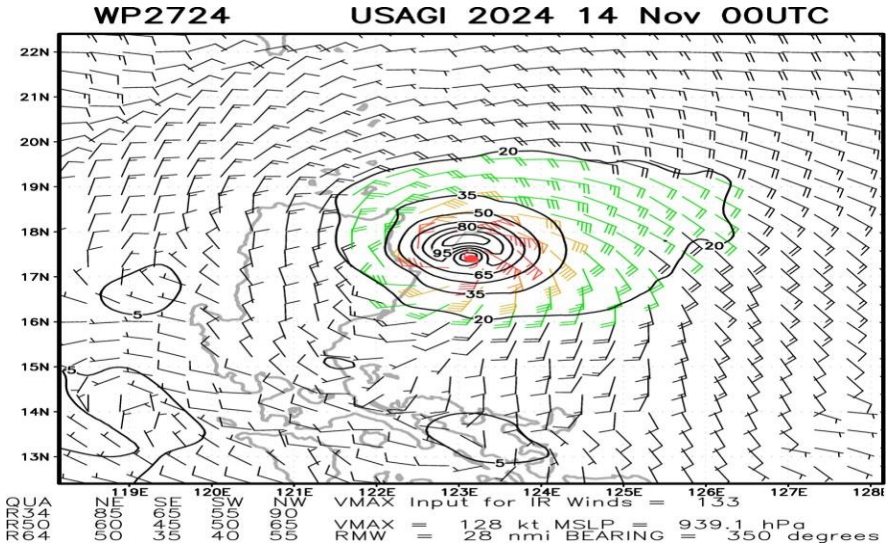

Fig. 13. Experimental version of the MTCSWA product for Typhoon Usagi valid 00 UTC 14 Nov. 2024. The product inputs are an IR-based 700 hPa wind field proxy, OSVW estimates from ASCAT, SMAP, SMOS, and AMSR2, low-level AMVs from Himawari-9, and nonlinear balanced winds based on AMSU core retrievals. Wind speed barbs and contours are in kts. [Credit: CIRA]

NOAA's university-based Cooperative Institutes produce several other integrated products in real-time demonstration mode. At CIRA for example, a compilation of several TC RMW estimates is provided for active TCs including experimental and documented methods discussed in Knaff et al., (2011), Chavas and Knaff, (2022), Avenas et al., (2024), and Tsukada and Horinouchi, (2023). Another example is a blended product developed by CIMSS is the Automated Rotational Center Hurricane Eye Retrieval (ARCHER, Wimmers and Velden, 2010), an objective algorithm that provides TC center fixes from multiple satellite platforms. In addition to center fixes, ARCHER also includes a retrieval of eye and core structure characteristics from LEO 85-91 GHz microwave observations (e.g., useful as input to M-PERC discussed in Section 3.4).

Another product developed at CIMSS and now used operationally at many global TC forecast centers is the satellite consensus (SATCON) TC intensity estimation algorithm (Velden and Herndon, 2020). The method objectively combines intensity estimates from several coincident automated IR and MW-based techniques to produce a consensus estimate that is more skillful than the individual estimates (example in Fig. 14). SATCON employs a weighting strategy that relies on the situational precision of each member and can provide valuable objective intensity estimates for post-storm assessments, especially in the absence of other data such as provided by reconnaissance aircraft. It can also serve as a near-real-time estimator of TC intensity for forecasters who can more quickly reconcile differences in various objective intensity methods and thus decrease the uncertainty and time spent on the intensity analysis. CIMSS produces publicly available near-real-time SATCON estimates for all global TCs (see Appendix A for the link).

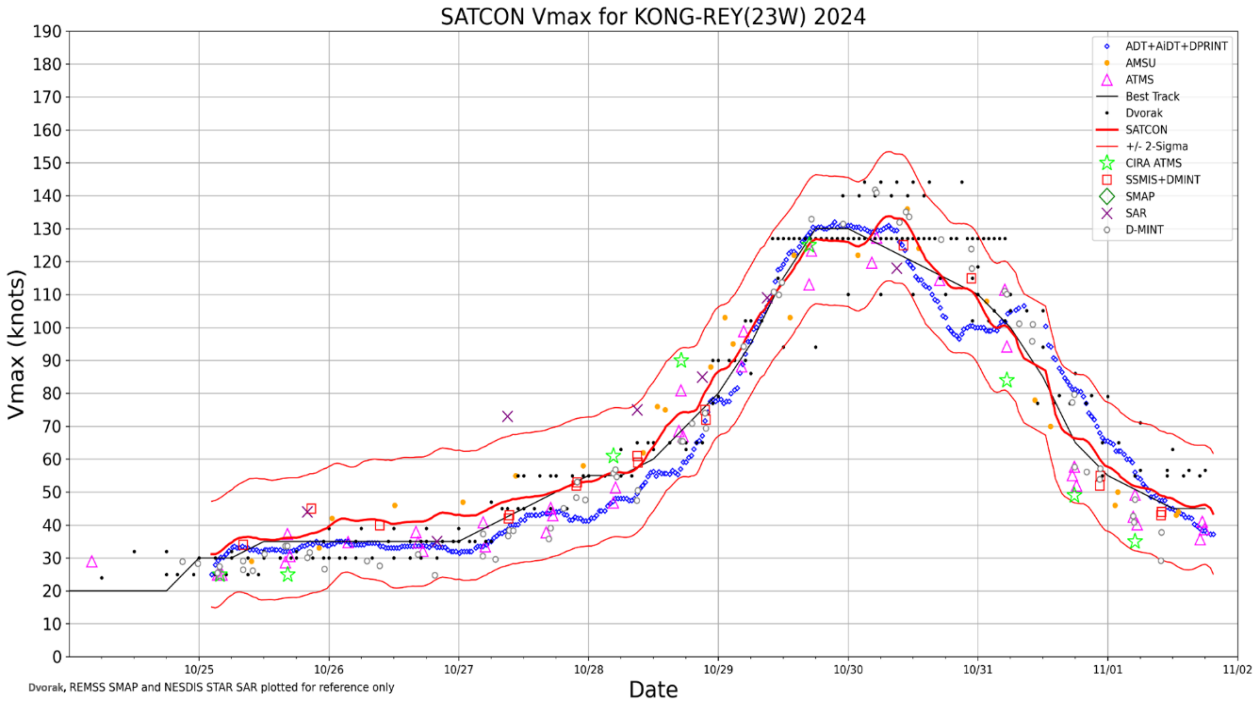

Fig. 14. SATCON product display for TC Kong-Rey (2024). Plotted are estimates of intensity (maximum 1-min. sustained wind, in kts) from various satellite-based sources along with the Best Track analysis from the Joint Typhoon Warning Center (black line). The bold red contour with attendant +/- 2-sigma confidence intervals (light red contours) is the SATCON weighted consensus of the estimates obtained from the methods/instruments shown in the upper right corner legend (except for Dvorak, SMAP and SAR that are currently not SATCON members). [Credit: CIMSS]

6. Satellite applications to 'Medicanes'

Early studies identified and characterized Medicanes based mostly on GEO VIS/IR imagery, as they bore a resemblance in appearance to hurricanes with an eye-like center and spiral cloud bands (Ernst and Matson, 1983; Reale and Atlas, 2001). Claud et al., (2010) first employed AMSU-A and -B to identify upper-level precursors, precipitation areas and deep convection associated with Medicanes. Since then, satellite-based diagnostic tools, combined with model-based studies and field experiments, have provided useful insights into the atmospheric processes associated with Medicanes' formation, evolution, and intensification (Miglietta et al., 2013; Dafis et al., 2018, 2020; Comellas et al., 2021). Active and PMW measurements from the NASA/JAXA GPM Core Observatory have enabled the analysis of Medicane precipitation structure evolution, also in relation to lightning activity (Marra et al., 2019; D'Adderio et al., 2022).

Other recent studies have focused on the Medicanes' TC-like warm core (WC) structure (Section 3.3), and the well-established methodology used for WC detection in TCs (Kidder et al., 2000; Brueske and Velden, 2003; Demuth et al., 2006; Herndon and Velden, 2012). It is the presence of this warm core thermal structure that places Medicanes close to TCs within the cyclone spectrum, similar to subtropical cyclones in other basins, permitting tools applied to TC analysis to be used to diagnose these systems. These tools have been applied to Medicanes' WC diagnostics for the first time by Panegrossi et al., (2023). The study analyses six Medicanes that occurred between 2014 and 2020, exploring the relationships between WC characteristics, deep convection (following Hong et al., 2005 and Funatsu et al., 2007), and cloud properties (cloud top height and ice water path estimates based on Rysman et al., 2021). Results suggest that such relationships link to not only the WC structure and strength, but also to the driving WC formation mechanism (e.g., diabatic vs. baroclinic processes). D'Adderio et al. (2024) further investigated this by analyzing two Medicanes that occurred in 2023, Helios and Juliette, using AMSU-A and ATMS-derived WCs evidencing very similar formation mechanisms for the two storms. The diagnostics of the WC and deep convection properties reveal differences in the two cyclones during their mature phase; a tropical transition (Juliette) vs. a warm seclusion (Helios). Expanding on this, Di Francesca et al. (2025) used satellite passive microwave data to analyze WC structure, deep convection, and an eye-like feature near the storm core for 23 candidate medicanes that occurred between 2000 and 2021. The study stratifies the cases into those that underwent a tropical transition and those that did not. As a result, while 13 cases exhibit a clear WC structure and closed eye feature, a true TC-like status is identified for 6 of them including Medicane Ianos in 2020 (Lagouvardos et al., 2022; Zimbo et al., 2022; Ferrarin et al., 2023; D'Adderio et al., 2022). These studies have been useful in providing the necessary diagnostic tools to discriminate between true Medicanes and storm systems that remain purely baroclinic or cold core. This is an important distinction that plays a role in the hazard communication messaging within the Mediterranean basin, as many systems called "Medicanes" in the past do not meet these newly identified thermal and structure definitions.

Medicane Ianos is used to illustrate how some of the satellite-based diagnostics tools can be employed for Medicane analysis. Around 12 UTC on 17 Sept. 2020, Figure 15 illustrates Tb imagery from the ATMS 54-55 GHz temperature sounding channels for WC identification and characterization, while Tb imagery from the 183 GHz channel shows the presence of spiraling rain band structure near an eye-like center. A cross-section through Medicane Ianos derived from ATMS thermal channel Tbs provides clear evidence of the presence of a WC anomaly. As Ianos approached the southwest coast of Greece, it reached peak intensity of 984 hPa and maximum

sustained 1-min. surface winds of near 44 ms^{-1} near landfall around 05 UTC on 18 Sept. (Lagouvardos et al., 2022). The intensity estimation algorithm developed at CIMSS based on WC Tb anomaly strength (developed for TCs) applied to Ianos yielded 980 hPa, and 32.4 ms^{-1} around 00:00 UTC on 18 Sept. The reasonable intensity estimates based on the Tb anomaly suggests that much like TCs, the WC is driving the low pressure. While storms that attain the intensity of Ianos are somewhat rare, this case shows that some storms in the basin acquire true TC status.

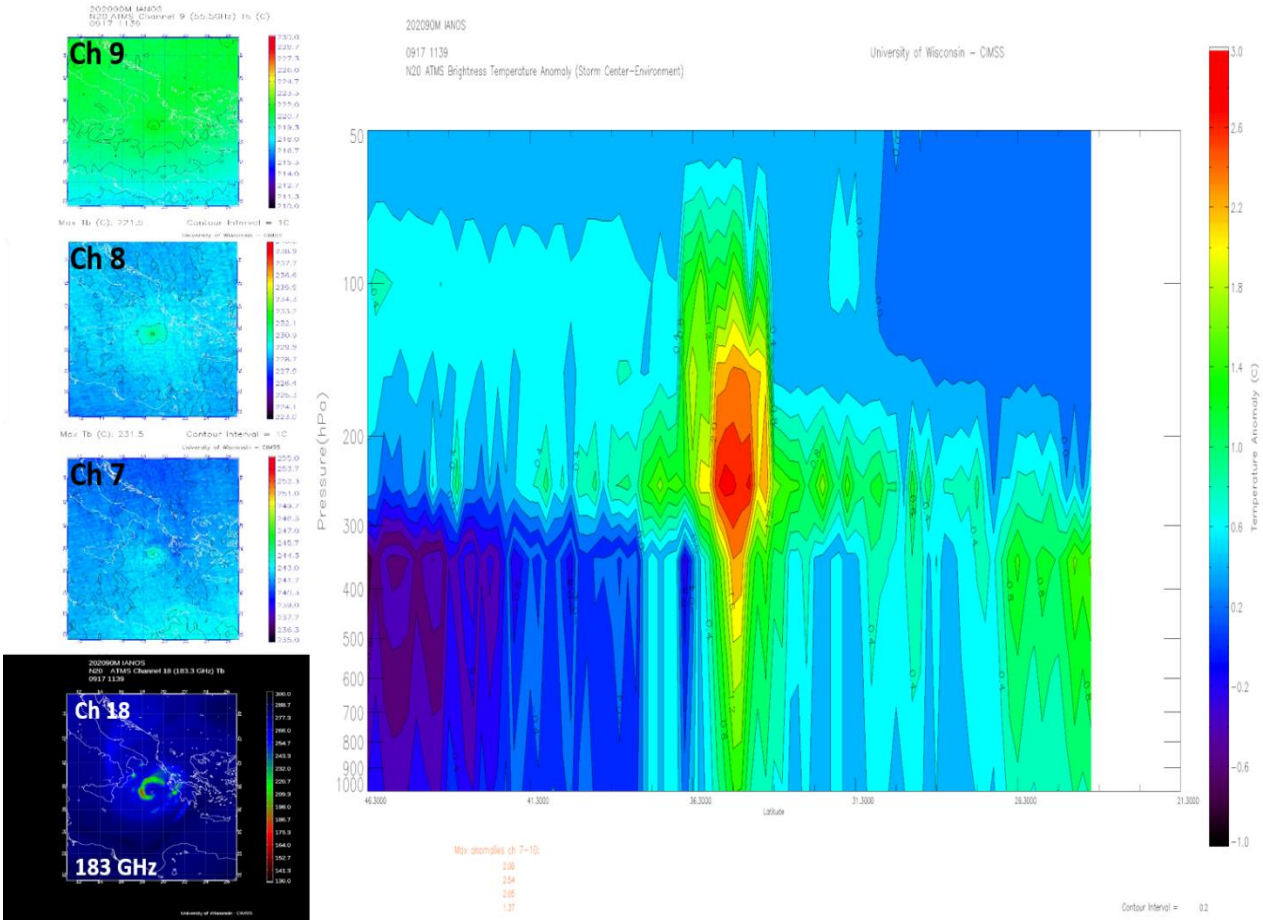

Fig. 15. View of Medicane Ianos from a NOAA-20 ATMS overpass at 11:39 UTC 17 Sept. 2020. Planar Tb views from the sounder thermal channels 7-9 on the left coincide with their approximate altitudes shown in Fig. 9. A longitudinal cross-section of Tb anomaly (deg. C) through the center of Ianos shows the warm-core structure similar to, but weaker than, its Super Typhoon Mawar counterpart shown in Fig. 9. The 183 GHz (channel 18) shows a ring of deep convection around the center of Ianos similar to an eyewall. [Credit: CIMSS]

Many of the other TC-focused, satellite-based tools discussed in this article could also be applied to the monitoring of Medicanes. From enhanced imagery (e.g., airmass, ProxyVis) to diagnostic products and algorithms (TPW for moisture analysis, OSVW for surface wind structure), satellite information can be crucial to augmenting the existing conventional observation network around the Mediterranean Sea for the analysis and forecasting of Medicanes.

7. Impacts of satellite data on model TC forecasts

7.1. Statistical-dynamical models

Statistical-dynamical TC intensity and rapid intensification (RI) forecast models input satellite information as predictors (e.g., DeMaria et al., 2005; Kaplan et al., 2010; Yamaguchi et al., 2018; Knaff et al., 2021). The revolution of more sophisticated analysis methods, i.e., most recently the surge in AI/ML techniques, has led to new models for RI prediction (Mercer et al., 2017; Xu et al., 2021; Slocum et al., 2023; 2024). Most of these efforts utilize GEO IR data due to timeliness and availability (Lagerquist et al., 2024). However, inspired by Cecil and Zipser, (1999), information based upon PMW (e.g., Jones et al., 2006; Su et al., 2020; Griffin et al., 2022) and satellite-based lightning (Slocum et al., 2023) show additional promise for improving intensity and RI forecasting. As skillful RI forecast methods become more numerous, partly due to increased use of new satellite data as predictors, objective consensus methods are also possible and showing skill (Sampson et al., 2023). These statistical-dynamical intensity and RI model forecasts remain competitive with hurricane-specific NWP model predictions and provide a stable baseline for TC forecasters.

7.2. Numerical weather prediction models

The significant impact of satellite data on modern global assimilation and NWP systems is well known. Over the last couple of decades, advances in data assimilation methods along with satellite remote sensing capabilities have led to notable increases in model forecast skill. For example, ECMWF first demonstrated significant forecast skill improvements resulting from cloudy-radiance assimilation (Geer et al., 2018). The introduction of new microwave sounder's (e.g., ATMS) information into operational systems has consistently led to an improvement in short and medium range forecast accuracy, including the effective assimilation of radiances (e.g., Bormann et al., 2013, 2019). Regarding TC forecasts, McNally et al., (2014) demonstrated the significant impact of polar-orbiting data on ECMWF model forecasts of Hurricane Sandy in 2012. In a very recent study, Magnusson et al. (2024) examined the impacts of various observation types on TC forecasts in the ECMWF system conducting observing system experiments (OSEs). The strongest impact came from withholding of all-sky microwave radiance observations, followed by scatterometer data. The impact for other satellite data such as GNSS-RO, AMVs and Aeolus were mixed/neutral, but they noted the AMV results were somewhat at odds with the more positive impacts found by Bormann et al. (2019).

Concerning regional TC models, Zhang et al., (2016, 2019), Honda et al., (2018), Minamide and Zhang, (2018) among others have shown the potential for further improving TC analysis and prediction through advanced ensemble assimilation of high-spatiotemporal all-sky infrared radiances from GEO. Furthermore, as shown and discussed in Section 2, high spatiotemporal AMV datasets produced from advanced GEO imagers with novel processing methodologies directed at capturing TC vortex-scale flows can benefit hurricane model analyses and forecasts (Wu et al., 2014; Velden et al., 2017; Sawada et al., 2019, 2020; Lewis et al., 2020; Li et al., 2020). These AMV datasets have also contributed to a myriad of diagnostic studies related to understanding TC behavior (Elsberry et al., 2018, 2020, 2023; Ryglicki et al., 2019, 2021; Tsujino et al., 2021).

8. The 'end user': Global TC analysis and forecast centers

Many national operational forecast centers and WMO mandated Regional Specialized Meteorological Centers (RSMCs) perform routine TC surveillance and analysis. A typical analysis (and sometimes forecast) cycle is performed every 6 hours but can be more frequent if conditions warrant (e.g. a major landfalling TC). Real-time operational TC monitoring leans heavily on satellite observations, especially in regions void of aerial reconnaissance. In fact, some agencies have trained satellite analysts who directly aid the TC specialists during the analysis cycle. The TC analysis steps can be loosely broken down as follows (along with key satellite-based imagery and products):

Step 1: **Pre-formation**

- Identify areas of potential TC development over region of responsibility (multispectral GEO animations, MIMIC-TPW, scatterometry, Saharan Air Layer products in the Atlantic basin)
- Continuously monitor suspect areas using above tools and LEO PMW imagery to look for circulation and sustained convective organization, which if found then triggers a transition to Step 2

Step 2: **TC analysis** (in addition to all available non-satellite inputs i.e., marine/coastal observations, radar, aircraft and NWP)

- For each identified area of sustained convective organization associated with low level circulation and continuing throughout TC lifecycle, generate regular position, intensity, structure and phase analyses
  - Position fixes (storm-centered and zoomed GEO IR/MSI, ProxyVis, LEO PMW, High-Res scatterometry/NRCS/ambiguities, SAR, ARCHER)
  - Intensity estimates (manual Dvorak technique based on GEO IR and VIS, objective intensity estimates based on IR, PMW and SATCON (mainly CIMSS), scatterometry, SAR/SMAP/AMSR2 wind speeds)
  - Structure/size analyses (2-D and quadrant surface wind radii including RMW) (scatterometry, SAR, SMAP, SMOS, MTCSWA, PMW imagery/MPERC)
  - Phase analysis (TC, ST, ET) (multispectral GEO, PMW sounder vertical x-sects)
  - Combine satellite fix information with all available conventional data, NWP data and continuity to determine an operational Best Track (position, intensity and structure)
  - Generate and transmit TC bulletins and essential data about the TC that can be used to initialize NWP models, including location, MSW, MSLP, and additional parameters like current storm speed/direction

A key analysis challenge for the operational TC center is synthesizing the range of inputs at standard times; many satellites and products provide irregular coverage. Data latency can be another issue. Despite these concerns, operational TC analysts are usually open to new and reliable

data sources as they become available, even if they are experimental. As the range of inputs to the analysis process increase, forecasters who are under time constraints appreciate collated information such as the regularly-updated CIMSS real-time product summary page (see Appendix A for link) which can save having to search for multiple sources of information.

9. Satellite applications to TC climate analyses and trends

In addition to real-time forecasting applications, satellite data is greatly aiding TC research. For example, nearly a half-century of satellite-based observations is allowing for climate applications. Current trends and projections of increased TC activity (based on theory and numerical climate models, most notably, stronger intensities) are often attributed to climate change (e.g. Sobel et al., 2016; Knutson et al., 2019, 2020). However, the confidence in this attribution can be jeopardized by temporal heterogeneities in the past observational records of TCs, i.e. the global "best track" records (Knapp and Kruk, 2010; Schreck et al., 2014). Even in the satellite era, gradual sensor improvements can lead to difficulties in identifying significant global trends in TC intensity over the past four decades. Kossin et al., (2013, 2020) attempt to address this by applying an objective TC intensity estimation algorithm (ADT) to a globally homogenized satellite data record (HURSAT, Knapp et al., 2011) to create a more temporally consistent record of TC intensity within the period 1982–2017. The HURSAT dataset provides 3-hourly GEO IR window channel (approximately 11 μm) images at the same spatial scale through time; all images being subsampled to ~8 km. While there have been improvements in GEO IR spatial resolutions (e.g., 8km down to 2 km), the resampling provides an attempt to homogenize the imagery for TC climate/trend purposes. The use of the objective ADT algorithm allows for consistency in the TC intensity analyses over time. The resulting trend analyses should serve to gain confidence in the projections of increased TC intensity under continued global warming.

The HURSAT dataset has also been used in other studies of TC size and TC eye climatologies (Knaff et al. 2014; Knapp et al., 2018), evaluation of model re-analyses (Kossin, 2015), and studies of cloud clusters (Zawislak and Zipser, 2010). HURSAT provides GEO imagery centered on TCs for the International Best Track Archive for Climate Stewardship (IBTrACS) dataset (Knapp et al., 2009). Other satellite-based datasets (e.g. PMW-based) have been used to create short-term TC climatologies (Lonfat et al., 2004; Wingo and Cecil, 2010; Qian et al., 2020; Yang et al., 2021; Guzman and Jiang, 2021 and many others). Most recently, the Tropical Cyclone Precipitation, Infrared, Microwave, and Environmental Dataset (TC PRIMED; Razin et al., 2023) provides a long-term (1987 – present) record of TC-centered PMW data. It is clear that satellite data, whether alone or integrated with other observations, has become an important climate analysis tool.

10. Emerging and planned satellites/sensors and data analysis techniques

10.1. WMO Integrated Global Observing System (WIGOS) core constellation satellites and instruments/sensors

The backbone of the global satellite-based observing system is the core constellation satellites (GEO and LEO) as determined by the WMO Commission for Observation, Infrastructure and Information Systems, and operated by a handful of national agencies (WMO, 2024b). The WIGOS core satellites constitute both legacy and cutting-edge new technologies to ensure both continuity and to meet the growing needs of the user communities. The WMO Observing Systems Capability Analysis and Review Tool (OSCAR, https://space.oscar.wmo.int/satellitestatuses/status) presents a great summary of the currently operating agency satellites and projected near-future missions.

Ricciardulli et al., (2023) nicely distills this information down to TC-relevant missions and sensors. Despite some challenges, such as the discontinuation of relied-upon sensors (SSMIS sounder, ASCAT-A, Windsat to name a few), or the desire for more high-resolution PMW imagers, it is easy to be optimistic about the remarkable new technologies that are emerging now and planned for the near future.

10.2. The new age of LEO smallsats/CubeSats and commercial sector ventures

Outside of the core constellation, there are a plethora of other existing and planned satellites and instruments of opportunity, most of which are also listed on the OSCAR website. Some of these are research, experimental or demonstrational missions with data latency and dissemination challenges. However, it has proven possible to overcome these impediments through unified efforts of the data providers, researchers and end user communities. A great example of this: NASA working with NOAA and other partners to make valuable new observation data from some of its Earth science missions (e.g., TRMM, GPM, TROPICS) available in near-real-time to global user communities. These demonstrational missions are often tomorrow's operational sensors.

The confluence of advanced antenna designs, instrument/sensor miniaturization, and the proliferation of commercial satellite launch opportunities is revolutionizing the satellite-based observing network. Smaller satellites and CubeSats (e.g., TROPICS, TEMPEST, RAINCUBE, GEMS, Tomorrow.io and others) are demonstrating cheaper alternatives to the legacy LEO satellites, although the latter will remain the backbone for years to come. As the commercial sector takes a seat at the satellite provider table, it will be vital to the integrity of future observations that there is compliance with standard agency practices concerning careful calibration, shared validation efforts, and cost-effective data dissemination policies. These will be important attributes as we enter the promising new age of commercial satellite launches, operations, and data buys.

10.3. Advancing satellite data processing/assimilation/analysis techniques and product displays

As the wealth of information from environmental satellites continues to skyrocket, there must be concurrent technologies to harbor and distill it into actionable products for user communities. This end-to-end process includes low-latency data ingest, computationally efficient processing, advanced assimilation methods and analysis tools, along with tailored product/information displays and dissemination for both research and operational communities.

Over the past decade or so, we have witnessed an explosion in AI machine learning techniques and applications to science problems. Implicit to these efforts is the need for high quality training datasets. The ability of AI methods to quickly churn on very large satellite data sets and produce robust analyses has led to new and improved TC applications (Pradhan et al., 2018; Wimmers et al., 2019; Chen et al., 2019; Lee et al., 2020; Zhuo and Tan, 2021; Higa et al., 2021; Griffin et al. 2022, and many others). As shown in Griffin et al., (2024), deep learning techniques applied to both IR and PMW multichannel data can produce highly competitive TC intensity estimates that operational TC forecast centers are already relying on. In another recent study, Wimmers et al., (2024) derives a two-dimensional surface wind field product for TC inner core domains based on a unique multi-branched U-Net model design with a loss function that efficiently compensates for the relative sparsity of labeled data. Reconnaissance aircraft flight-level in situ winds from center-crossing transects and matching PMW and IR imagery are used in training the model to reproduce a full two-dimensional field of flight-level wind, which can then be subject to surface-level reduction factors to create the surface wind field product. In a final step, the 2-D wind field profiles are normalized by a concurrent D-MINT model intensity (max surface wind) estimate (Griffin et

al., 2024). The results indicate that even challenging TC inner-core radial horizontal wind profiles including eyewall maxima and secondary outer maxima are reasonably captured by the product, and the model performs well in a variety of environments including strong vertical wind shear. Shown in Figure 16 is an example output display, which captures the rapidly changing inner core structure of Hurricane Kirk over a 12-hr period under increasing vertical wind shear.

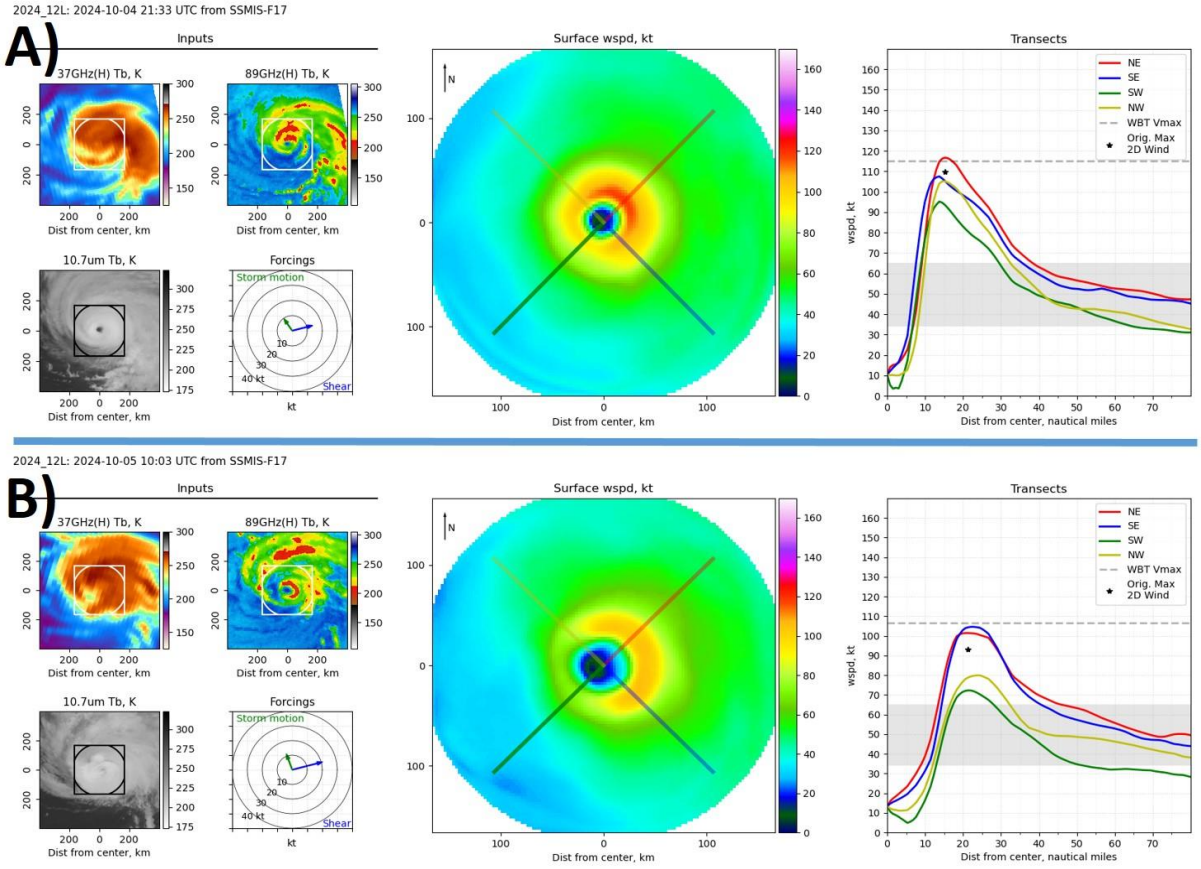

Fig. 16. Hurricane Kirk inner-core surface wind fields produced from the deep learning method of Wimmers et al., (2024), for A) 2133 UTC on 4 Oct., and B) 1003 UTC on 5 Oct. 2024. Input data (left panels) consists of SSMIS 37 and 89 GHz Tb, and 10.7 μm Tb from GOES-16, along with estimates of storm motion and environmental shear. The middle panels show the color-coded (by wind speed, in kts) 2-D surface wind field following the procedure described in Wimmers (2025). The right-hand panels depict the horizontal radial wind profiles along the 4 quadrant transects depicted in the middle panels, along with the model and NHC working best track (WBT) maximum surface wind estimates. [Credit: A. Wimmers, CIMSS]

11. Summary

Tropical cyclones and Medicanes are extreme weather hazards well known for their occasional devastating impacts on life and property. As populations and infrastructure built along coastlines grow, they are prone to an increasing threat from landfall impacts. While some prone regions are fortunate to benefit from reconnaissance aircraft surveillance, the majority of these storms spend most of their lifecycle over marine environments lacking in conventional observations. Thus, satellite-based remote sensing applications can play a crucial role in monitoring and analyzing key storm characteristics critical to the forecast process.

This review represents only a sample of significant recent advances in satellite remote sensing capabilities and applications to the analysis and forecasting of high-impact weather events such as TCs and Medicanes. Readers are encouraged to peruse another excellent summary of recent remote sensing advances in TC analysis presented in Ricciardulli et al., (2023), with more focus on the polar orbiting sensors such as C-band SARs, L-band and combined C/X-band radiometers, scatterometers, and microwave imagers/sounders. In addition, the excellent summary reports of the four WMO IWSATC meetings held to date, along with the delegate presentations and recordings are accessible here. Finally, the internet is full of informative websites pertaining to satellite applications of TCs; links to some of them appear in Appendix A.

There are still unaddressed scientific challenges concerning TC and Medicane formation and intensification processes, and about forecasting capabilities to better predict their impacts at regional and local scales (especially in terms of substantial rainfall, winds, and storm surges). This requires an integrated approach between modeling and observational communities, including satellite-based remote sensing, and operational forecast centers supported by solid research and technology development. Exploitation of exciting new satellite sensors and data analysis approaches that are emerging now and in the near future will ensure the continued advancement of satellite-based applications to TCs and Medicanes.

Acknowledgements

The authors would like to acknowledge the global satellite agencies and institutes that make their data freely available and in a timely manner for TC analysis. Contributions to this article were supported by NOAA/NESDIS base funding (Knaff), by NOAA grant NA19OAR4320073-T1-01 and the Office of Naval Research grant N00014-21-1-2112 (Tsukada), the Office of Naval Research grant N00014-21-1-2130 (Hawkins), and the ESA Medicanes project ESA Contract No. 4000144111/23/I-KE (Panegrossi).

Appendix A – Selection of active TC satellite applications and products web sites

https://www.ospo.noaa.gov/products/ocean/tropical/ NOAA Office of Satellite and Products Operations (OSPO), real time operational TC products

https://tropic.ssec.wisc.edu/tropic.php Univ. Wisconsin-CIMSS TC Research Group real-time and archived TC satellite imagery and products

https://rammb2.cira.colostate.edu/research/tropical-cyclones/ NOAA Regional and Mesoscale Meteorology Branch (RAMMB) at Colorado St. Univ.-CIRA satellite-based TC research products

https://science.nrlmry.navy.mil/geoips/tcweb/active/ U.S. Naval Research Lab. at Monterey, California satellite imagery of TCs with a focus on microwave products

https://www.remss.com/tropical-cyclones/tc-winds/ Remote Sensing Systems (REMSS) TC products with a focus on ocean surface wind vector algorithms and products

https://www.tropicaltidbits.com/sat/ A user-supported site developed by Levi Cowan, currently a TC forecaster at the Joint Typhoon Warning Center. The site includes TC-focused satellite imagery.

https://www.star.nesdis.noaa.gov/socd/mecb/sar/sarwinds_tropical.php NOAA/NESDIS SAR near real-time TC overpass acquisitions and derived products (OSVW)

https://scatterometer.knmi.nl/home/ Royal Netherlands Meteorological Institute (KNMI) near real-time and archived OSVW products for all C- and Ku-band scatterometers

https://manati.star.nesdis.noaa.gov/products.php NOAA/NESDIS site with a myriad of near real-time and archived OSVW products

https://www.ospo.noaa.gov/products/atmosphere/precipitation.html NOAA/NESDIS near real-time satellite-based moisture and precipitation products

https://rammb-data.cira.colostate.edu/tcprimed/#microwave NOAA/CSU TC PRecipitaion, Infrared, Microwave and Environmental Dataset (TC Primed) is a consolidated archive of TC products

https://eo4society.esa.int/projects/medicanes/ European Space Agency Medicanes project summary information

Appendix B – List of acronyms/abbreviations

ABI Advanced Baseline Imager

ADT Advanced Dvorak Technique

AHI Advanced Himawari Imager

AI Artificial Intelligence

ALADIN Atmospheric Laser Doppler INstrument

ALOS Advanced Land Observing Satellite

ALPW Advective Layered Precipitable Water

AMSR Advanced Microwave Scanning Radiometer

AMSU Advanced Microwave Sounding Unit

AMV Atmospheric Motion Vector

ARCHER Automated Rotational Center Hurricane Eye Retrieval

ASCAT Advanced SCATterometer

ASWind AMV-based Sea-surface Winds

ATCF Automated Tropical Cyclone Forecasting

ATL Atlantic (basin)

ATMS Advanced Technology Microwave Sounder

AWIPS Advanced Weather Interactive Processing System

BT Best Track

CDO Central Dense Overcast

CIMR Copernicus Imaging Microwave Radiometer

CIMSS Cooperative Institute for Meteorological Satellite Studies

CIRA Cooperative Institute of Research in the Atmosphere

CMA Chinese Meteorological Administration

CMORPH Climate Prediction Center MORPHing technique

CNN Convolutional Neural Networks

COSMIC Constellation Observing System for Meteorology Ionosphere and Climate

COWVR Compact Ocean Wind Vector Radiometer

CSA Canadian Space Administration

CYGNSS Cyclone Global Navigation Satellite System

DL Deep Learning

DMINT Deep Microwave INtensity of Tropical cyclones

DMSP Defense Meteorological Satellite Program

DPRINT DeeP infraRed INtensity of Tropical cyclones

DWL Doppler Wind Lidar

ECMWF European Centre for Medium-Range Weather Forecasts

EOS Earth Observation Satellite (India)

ERC Eyewall Replacement Cycle

ESA European Space Agency

ET Extra-Tropical

eTRAP ensemble Tropical RAinfall Potential

EUMETSAT European Organization for the Exploitation of Meteorological Satellites

FY FengYun (China)

GCOM-W Global Change Observation Mission for Water

GEMS Global Environmental Monitoring System

GEO Geostationary Earth Orbit

GHz GigaHertz

GMI GPM Microwave Imager

GMS Geostationary Meteorological Satellite (Japan)

GNSS Global Navigation Satellite System

GNSS-RO GNSS Radio Occultation

GOES Geostationary Operational Environmental Satellite (U.S.)

GOSAT-GW Global Observation SATellite for Greenhouse gases and Water cycle

GPM Global Precipitation Mission

GPS Global Positioning System

HISA Hurricane Intensity and Structure Algorithm

H-pol Horizontal polarization

HRD Hurricane Research Division

HSCAT Haiyang SCATterometer

HURSAT HURricane SATellite (dataset)

HWRF Hurricane Weather Research and Forecasting model

HY-2A HaiYang-2A satellite

IBTrACS International Best Track Archive for Climate Stewardship

IFREMER Institut Français de Recherche pour l'Exploitation de la Mer (French Inst. for Ocean Science)

IMD Indian Meteorological Department

IMERG Integrated Multi-satellitE Retrievals for GPM

INSAT Indian National SATellite system

IR Infrared

ISRO Indian Space Research Organization

ISS International Space Station

IWSATC International Workshop on Satellite Analysis of Tropical Cyclones

JASON Joint Altimetry Satellite Oceanography Network

JAXA Japanese Aerospace Exploration Agency

JMA Japan Meteorological Agency

JPL Jet Propulsion Laboratory

JPSS Joint Polar Satellite System

JTWC Joint Typhoon Warning Center

KNMI Koninklijk Nederlands Meteorologisch Instituut (Royal Dutch Meteorological Institute)

KOMPSAT KOrean MultiPurpose SATellite

LEO Low Earth Orbit

McIDAS Man-computer Interactive Data Access System

Medicane Mediterranean hurricane

MetOp Meteorological Operational satellite (EUMETSAT)

MetOp-SG MetOp-Second Generation

MIMIC-TC Morphed Integrated Microwave Imagery at CIMSS-TC

MIMIC-TPW Morphed Integrated Microwave Imagery at CIMSS-TPW

ML Machine Learning

MPERC Microwave Probability of Eye Replacement Cycle

MSG Meteosat Second Generation

MSI MultiSpectral Imagery

MSLP Minimum Sea Level Pressure

MSW Maximum Sustained Winds

MTCSWA Multi-platform Tropical Cyclone Surface Wind Analysis

MTG MeteoSat Third Generation

MW Microwave

MWHTS MicroWave Humidity and Temperature Sounder

MWRI MicroWave Radiometer Imager

NASA National Aeronautics and Space Administration

NCEP National Centers for Environmental Prediction

NESDIS National Environmental Satellite, Data, and Information Service

NHC National Hurricane Center

NISAR NASA-ISRO Synthetic Aperture Radar

NOAA National Oceanic and Atmospheric Administration

NPP National Polar-orbiting Partnership

NRCS Normalized Radar Cross Section

NRL-MRY Naval Research Laboratory at Monterey

NRT Near Real-Time

NSOAS National Satellite Ocean Applications Service (China)

NWP Numerical Weather Prediction

OHC Ocean Heat Content

OSCAR Observing Systems Capability Analysis and Review tool

OSCAT OceanSat SCATterometer

OSE Observing System Experiment

OSPO Office of Satellite and Products Operations (NOAA/NESDIS)

OSVW Ocean Surface Vector Winds

PALSAR Phased Array L-band Synthetic Aperture Radar

PMW Passive MicroWave

RainCube Radar in a CubeSat

RCM Radarsat Constellation Mission

REMSS Remote Sensing Systems

RI Rapid Intensification

RMW Radius of Maximum Wind

RSMC Regional Specialized Meteorological Center

SAL Saharan Air Layer

SAR Synthetic Aperture Radar

SATCON SATellite CONsensus

SCA SCAtterometer (MetOp)

SEF Secondary Eye Formation

SFMR Stepped Frequency Microwave Radiometer

SHOC Satellite Hurricane Observation Campaign

SMAP Soil Moisture Active and Passive

SMOS Soil Moisture and Ocean Salinity

SSMIS Special Sensor Microwave Imager/Sounder

SST Sea Surface Temperature

STAR SaTellite Applications and Research (NOAA/NESDIS)

Tb brightness Temperature

TC Tropical Cyclone

TCFP Tropical Cyclone Formation Product

TEMPEST TEMPoral Experiment for Storm and Tropical systems

TIROS Television InfraRed Observation Satellites

TMI TRMM Microwave Imager

TOPEX TOPography EXperiment

TPW Total Precipitable Water

TRMM Tropical Rainfall Measurement Mission

TROPICS Time-Resolved Observations of Precipitation and storm Intensity with a Constellation of Smallsats

UTC Coordinated Universal Time

VH/HV Vertical transmit and Horizontal receive/Horizontal transmit and Vertical receive

VIS Visible

V-pol Vertical polarization

WBT Working Best Track

WC warm core

WIGOS WMO Integrated Global Observing System

WMO World Meteorological Society

WSF-M Weather System Follow-on - Microwave

References

Alpers, W., Z. Yuan, A. Mouche, and P. W. Chan, 2021: A note on radar signatures of hydrometeors in the melting layer as inferred from Sentinel-1 SAR data acquired over the ocean. *Remote Sensing of Environment*, **253**(10p), 112177. https://doi.org/10.1016/j.rse.2020.112177

Alsweiss, S., J. Sapp, Z. Jelenak, P. Chang, 2021: An operational all-weather wind speed from AMSR2. *IEEE International Geoscience and Remote Sensing Symposium IGARSS*. Presented at the IGARSS IEEE International Geoscience and Remote Sensing Symposium, IEEE, Brussels, Belgium, pp. 7334-7337. 10.1109/IGARSS47720.2021.9553710

Alsweiss, S., S. Soisuvarn, Z. Jelenak, P. S. Chang and C. R. Jackson, 2024: Estimating Tropical Cyclones Wind Radii Using NOAA ASCAT Ultra High-Resolution Measurements. Proceedings IGARSS 2024 IEEE International Geoscience and Remote Sensing Symposium, Athens, Greece, pp. 5807-5809. https://doi.org/10.1109/IGARSS53475.2024.10641502 .

Avenas, A., A. Mouche, P. Tandeo, J. Piolle, D. Chavas, R. Fablet, J. Knaff, and B. Chapron, 2023: Reexamining the Estimation of Tropical Cyclone Radius of Maximum Wind from Outer Size with an Extensive Synthetic Aperture Radar Dataset. *Mon. Wea. Rev.*, **151**, 3169-3189. https://doi.org/10.1175/MWR-D-23-0119.1

Avenas, A., Chapron, B., Mouche, A. Paul Platzer and L. Vinour, 2024: Revealing short-term dynamics of tropical cyclone wind speeds from satellite synthetic aperture radar. *Sci. Rep.* ***14***, 12808. https://doi.org/10.1038/s41598-024-61384-w.

Bessho, K., T. Nakazawa, S. Nishimura, and K. Kato, 2010: Warm Core Structures in Organized Cloud Clusters Developing or Not Developing into Tropical Storms Observed by the Advanced Microwave Sounding Unit. *Mon. Wea. Rev.*, **138**, 2624–2643. https://doi.org/10.1175/2010MWR3073.1.

Blackwell, W., S. Braun, R. Bennartz, C. Velden, M. DeMaria, R. Atlas, J. Dunion, F. Marks, R. Rogers, B. Annane, R. V. Leslie, 2018: An overview of the TROPICS NASA Earth Venture Mission. *QJRMS*, **144**, Issue 1, 16-26. https://doi.org/10.1002/qj.3290

Bormann, N., A. Fouilloux and W. Bell, 2013: Evaluation and assimilation of ATMS data in the ECMWF system. *J. Geophys. Res.*, **118**, no. 23, 2970-12980.

Bormann, N., H. Lawrence, and J. Farnan, 2019: Global Observing System Experiments in the ECMWF Assimilation System. *ECMWF Tech Memo* **839**. https://www.ecmwf.int/en/elibrary/80953-global-observing-system-experiments-ecmwf-assimilation-system

Boukabara, S. et al., 2011: MiRS: An All-Weather 1DVAR Satellite Data Assimilation and Retrieval System. *IEEE Transactions on Geoscience and Remote Sensing*, **49**(9), 3249–3272. [10.1109/tgrs.2011.2158438]

Brueske, K. F., and C. S. Velden, 2003: Satellite-based tropical cyclone intensity estimation using the NOAA-KLM series Advanced Microwave Sounding Unit. *Mon. Wea. Rev.*, **131**, 687-697.

Cecil, D. J., and E. J. Zipser, 1999: Relationships between Tropical Cyclone Intensity and Satellite-Based Indicators of Inner Core Convection: 85-GHz Ice-Scattering Signature and Lightning. *Mon. Wea.Rev.*, **127**,103–123. https://doi.org/10.1175/1520-0493(1999)127<0103:RBTCIA>2.0.CO;2.

Chavas, D. R., and J. A. Knaff, 2022: A simple model for predicting the tropical cyclone radius of maximum wind from outer size. *Wea. Forecasting*, **37**, 563-579. https://doi.org/10.1175/WAF-D-21-0103.1

Chen, B., B. Chen, H. Lin, and R. L. Elsberry, 2019: Estimating Tropical Cyclone Intensity by Satellite Imagery Utilizing Convolutional Neural Networks. *Wea. Forecasting*, **34**, 447–465. https://doi.org/10.1175/WAF-D-18-0136.1.

Chirokova, G., et al., 2023: ProxyVis – a Proxy for Nighttime Visible Imagery Applicable to Geostationary Satellite Observations. *Wea. Forecasting*, **38**, 2527-2550. https://doi.org/10.1175/WAF-D-23-0038.1.

Claud, C., Alhammoud, B., Funatsu, B. M., and Chaboureau, J.-P., 2010: Mediterranean hurricanes: large-scale environment and convective and precipitating areas from satellite microwave observations. *Nat. Hazards Earth Syst. Sci.,* **10**, 2199–2213. https://doi.org/10.5194/nhess-10-2199-2010.

Combot, C., A. Mouche, J. A. Knaff, Y. Zhao, Y. Zhao, L. Vinour, Y. Quilfen, and B. Chapron, 2020a: Extensive high-resolution Synthetic Aperture Radar (SAR) data analysis of tropical cyclones: Comparisons with SFMR flights and best track. *Mon. Wea. Rev*., **148**(11), 4545–4563, https://doi.org/10.1175/MWR-D-20-0005.1.

Combot, C., Y. Quilfen, Yves, A. Mouche, J. Gourrion, C. de Boyer Montégut, B. Chapron, Bertrand and J. Tournadre, 2020b: Space-based observations of surface signatures in the wakes of the 2018 Eastern Pacific tropical cyclones. *Journal of Operational Oceanograph*y. **13,** S132-S137.

Comellas Prat, A.; Federico, S.; Torcasio, R.C.; D'Adderio, L.P.; Dietrich, S.; Panegrossi, G., 2021: Evaluation of the Sensitivity of Medicane Ianos to Model Microphysics and Initial Conditions Using Satellite Measurements. *Remote Sens.,* **13**, 4984-4998. https://doi.org/10.3390/rs13244984

D'Adderio L.P., D. Casella, S. Dietrich, P. Sanò, G. Panegrossi, 2022: GPM-CO observations of Medicane Ianos: Comparative analysis of precipitation structure between development and mature phase, *Atmos. Res*., **273.** https://doi.org/10.1016/j.atmosres.2022.106174.

D'Adderio, L.P., G. Panegrossi, S. Dafis, J.-F. Rysman, D. Casella, P. Sanò, A. Fuccello, M. M. Miglietta, 2024: Helios and Juliette: Two falsely acclaimed Medicanes?, *Atmospheric Research*, **299**, 107179, ISSN 0169-8095. https://doi.org/10.1016/j.atmosres.2023.107179.

Di Francesca, V., L. P. D'Adderio, P. Sanò, J.-F. Rysman, D. Casella, and G. Panegrossi, 2025: Passive microwave-based diagnostics of Medicanes over the period 2000–2021, *Atmospheric Research*, **316**, 107922, ISSN 0169-8095, https://doi.org/10.1016/j.atmosres.2025.107922.

Dafis, S., Rysman, J.F., Claud, C., Flaounas, E., 2018. Remote sensing of deep convection within a tropical-like cyclone over the Mediterranean Sea. *Atmospheric Science Letters*, **19**, e823.

Dafis S., Claud, C., Kotroni, V., Lagouvardos K., Rysman J-F., 2020: Insights into the convective evolution of Mediterranean tropical-like cyclones. *Q J R Meteorol Soc*. 2020; **146**: 4147–4169. https://doi.org/10.1002/qj.3896

Davis, C.A., Bosart, L. F., 2003: Baroclinically Induced Tropical Cyclogenesis. *Mon. Weather Rev*., **131**, 2730–2747.

DeMaria, M., M. Mainelli, L. K. Shay, J. A. Knaff, and J. Kaplan, 2005: Further Improvements to the Statistical Hurricane Intensity Prediction Scheme (SHIPS). *Wea. Forecasting*, **20**, 531–543. https://doi.org/10.1175/WAF862.1.

Demuth, J. L., M. DeMaria, and J. A. Knaff, 2006: Improvement of Advanced Microwave Sounding Unit Tropical Cyclone Intensity and Size Estimation Algorithms. *J. Appl. Meteor. Climatol.*, **45**, 1573–1581. https://doi.org/10.1175/JAM2429.1.

Ditchek, S. D., J. Molinari, K. L. Corbosiero, and R. G. Fovell, 2019: An objective climatology of tropical cyclone diurnal pulses in the Atlantic basin. *Mon. Wea. Rev.*, **147**, 591–605. https://doi.org/10.1175/MWR-D-18-0368.1.

Dunion, J. P., C. D. Thorncroft, and C. S. Velden, 2014: The tropical cyclone diurnal cycle of mature hurricanes. *Mon. Wea. Rev.,* **142**, 3900–3919. https://doi.org/10.1175/MWR-D-1300191.1.

Dunion, J.P., and C.S. Velden, 2004: The impact of the Saharan Air Layer on Atlantic tropical cyclone activity. *Bull. Amer. Meteor. Soc.*, **85,** no. 3, 353-365.

Dvorak, V., 1975: Tropical cyclone intensity analysis and forecasting from satellite imagery *Mon. Wea. Rev*., **103**, pp. 420-430, 10.1175/1520-0493(1975)103<0420:TCIAAF>2.0.CO;2

Dvorak, Vernon F. (1984). Tropical cyclone intensity analysis using satellite data. *NOAA technical report NESDIS* **11.** https://repository.library.noaa.gov/view/noaa/19322

Ebert, E. E., M. Turk, S. J. Kusselson, J. Yang, M. Seybold, P. R. Keehn, and R. J. Kuligowski, 2011: Ensemble Tropical Rainfall Potential (eTRaP) forecasts. *Wea. Forecasting*, **26**, 213-224. https://doi.org/10.1175/2010WAF2222443.1

Elsberry, R. L., E. A. Hendricks, C. S. Velden, M. M. Bell, M. Peng, E. Casas, and Q. Zhao, 2018: Demonstration with special TCI-15 datasets of potential impacts of new-generation satellite atmospheric motion vectors on Navy regional and global models. *Wea. Forecasting*, **33**, 1617–1637. https://doi.org/10.1175/WAF-D-17-0168.1.

Elsberry, R. L., J. W. Feldmeier, H.-J. Chen, M. Peng, C. S. Velden, and Q. Wang, 2020: Challenges and opportunities with new generation geostationary meteorological satellite datasets for analyses and initial conditions for forecasting Hurricane Irma (2017) rapid intensification event. *Atmosphere*, **11**, 1200-1217. https://doi.org/10.3390/atmos11111200.

Elsberry, R. L., J. W. Feldmeier, H. Chen, and C. S. Velden, 2023: High Temporal Resolution Analyses with GOES-16 Atmospheric Motion Vectors of Mesovortex Rapid Intensification in Subtropical Cyclone Henri (2021). *Wea. Forecasting*, **38**, 1173–1194. https://doi.org/10.1175/WAF-D-22-0148.1.

Emanuel, K.A., 1988: The maximum intensity of hurricanes. *J. Atmos. Sci*., **45**, 1143-1155.

Entekhabi, D., et al., 2014: SMAP Handbook. National Aeronautics and Space Administration. https://smap.jpl.nasa.gov/system/internal_resources/details/original/178_SMAP_Handbook_FINAL_1_JULY_2014_Web.pdf.

Entekhabi, D., and co-authors, 2010: The soil moisture active passive (SMAP) mission. *Proc. IEEE 98*, 704e716. https:// doi.org/10.1109/JPROC.2010.2043918.

Ernst, J., M. Matson, 1983: A Mediterranean tropical storm? *Weather*, **28**, 332-337. https://doi.org/10.j.1477-8696.1983.tb04818.x

EUMETSAT, 2021: https://osi-saf.eumetsat.int/community/stories/wind-scatterometer-constellation-captures-landfall-hurricane-ida

Ferrarin, C., and co-authors, 2023: Assessing the coastal hazard of Medicane Ianos through ensemble modelling. *Nat. Hazards Earth Syst. Sci*., **23**, 2273–2287. https://doi.org/10.5194/nhess-23-2273-2023.

Flaounas, E., Gray, S. L., and Teubler, F., 2021: A process-based anatomy of Mediterranean cyclones: from baroclinic lows to tropical-like systems. *Weather Clim. Dynam*., **2**, 255–279. https://doi.org/10.5194/wcd-2-255-2021.

Forsythe, J. M., S. Q. Kidder, K. K. Fuell, A. LeRoy, G. J. Jedlovec, and A. S. Jones, 2015: A multisensor, blended, layered water vapor product for weather analysis and forecasting. *NWA Journal of Operational Meteor*., **3**, 5, 41-58.

Funatsu, B. M., C. Claud, and J.-P. Chaboureau, 2007: Potential of Advanced Microwave Sounding Unit to identify precipitating systems and associated upper-level features in the Mediterranean region: Case studies. *J. Geophys. Res.*, **112**, D17113. https://doi.org/10.1029/2006JD008297.

Garrett, K., H. Liu, K. Ide, R. Hoffman, K. Lukens, 2022: Optimization and impact assessment of Aeolus HLOS wind assimilation in NOAA's global forecast system. *Q J R Meteorol Soc*., **148**, 2703–2716. https://doi.org/10.1002/qj.4331

Geer, A., and Coauthors, 2018: All-sky satellite data assimilation at operational weather forecasting centres. *QJRMS*, **144**, 1191-1217. https://doi.org/10.1002/qj.3202

Goni G., K., Garzoli S., Olson D., 1996: Dynamics of the Brazil-Malvinas confluence based on inverted echo sounders and altimetry. *J Geophys., Res*., **101**, 16273–16289.

Goni, G. et al., 2009: Applications of Satellite-Derived Ocean Measurements to Tropical Cyclone Intensity Forecasting. *Oceanography,* **22**(3), 190-197.

Goodman, S. J., and Coauthors, 2012: The GOES-R Proving Ground: Accelerating User Readiness for the Next-Generation Geostationary Environmental Satellite System. *Bull. Amer. Meteor. Soc.*, **93**, 1029–1040. https://doi.org/10.1175/BAMS-D-11-00175.1.

Griffin, S. M., 2017: Climatology of Tropical Overshooting Tops in North Atlantic Tropical Cyclones. *J. Appl. Meteor. Climatol.*, **56**, 1783–1796. https://doi.org/10.1175/JAMC-D-16-0413.1.

Griffin, S. M., A. Wimmers, and C. S. Velden, 2022: Predicting Rapid Intensification in North Atlantic and Eastern North Pacific Tropical Cyclones Using a Convolutional Neural Network. *Wea. Forecasting*, **37**, 1333–1355. https://doi.org/10.1175/WAF-D-21-0194.1.

Griffin, S. M., A. Wimmers, and C. S. Velden, 2024: Predicting Short-Term Intensity Change in Tropical Cyclones Using a Convolutional Neural Network. *Wea. Forecasting*, **39**, 177–202. https://doi.org/10.1175/WAF-D-23-0085.1.

Guo C., Ai W., Hu S., Du X. and Chen N., 2022: Effect of precipitation on synthetic aperture radar hurricane wind field retrieval. *Front. Environ. Sci.* **10**:1034045. https://doi.org/10.3389/fenvs.2022.1034045

Guzman, O. and H. Jiang, 2021: Global Increase in Tropical Cyclone Rain Rate. *Nat. Commun*. **12**, 5344. https://doi.org/10.1038/s41467-021-25685-2.

Hawkins, J.D., T. F. Lee, F. J. Turk, K. L. Richardson, C. R. Sampson, and J. E. Kent, 2004: The NRL tropical cyclone R&D web page upgrades. 26th AMS Conf. Hurr. Trop. Meteor, https://ams.confex.com/ams/26HURR/techprogram/paper_75987.html.

Hawkins, J. D. and C. Velden, 2011: Supporting meteorological field experiment missions and post-mission analysis with satellite digital data and products. *Bull. Amer. Meteor. Soc*., **92**, 1009-1022.

Hawkins, J., C. Velden and co-authors, 2025: A Historical Perspective on Tropical Cyclone Characterization via the DMSP Sensor Suite. *BAMS*, in review.

Haynes, K., C. Slocum, J. Knaff, K. Musgrave, I. Ebert-Uphoff 2022: Aiding Tropical Cyclone Forecasting by Simulating 89-GHz Imagery from Operational Geostationary Satellites. *Preprints 21st Conference on Artificial Intelligence for Environmental Science*, Boston, MA (2022). https://ams.confex.com/ams/102ANNUAL/exhibits.cgi/Paper/394364

Herndon, D. and Velden, C. S., 2012: Estimating tropical cyclone intensity using SSMIS and ATMS sounders**.** Conference on Hurricanes and Tropical Meteorology. *Preprints 30th Hurr. Trop. Meteor.*, Ponte Vedra Beach, FL, Amer. Meteor. Soc.

Higa, M., Tanahara, S., Adachi, Y. et al., 2021: Domain knowledge integration into deep learning for typhoon intensity classification. *Sci Rep* **11**, 12972. https://doi.org/10.1038/s41598-021-92286-w

Honda, T., and Coauthors, 2018: Assimilating all-sky Himawari-8 satellite infrared radiances: A case of Typhoon Soudelor (2015). *Mon. Wea. Rev.*, **146**, 213–229. https://doi.org/10.1175/MWR-D-16-0357.1.

Hong, G., G. Heygster, J. Miao, and K. Kunzi, 2005: Detection of tropical deep convective clouds from AMSU-B water vapor channels measurements, J. *Geophys. Res.*, **110**, D05205. doi:10.1029/2004JD004949.

Horinouchi, T., Tsujino, S., Hayashi, M., Shimada, U., Yanase, W., Wada, A., & Yamada, H., 2023: Stationary and transient asymmetric features in tropical cyclone eye with wavenumber-1 instability: Case study for Typhoon Haishen (2020) with atmospheric motion vectors from 30-second imaging. *Monthly Weather Review*, **151**(1), 253–273. https://doi.org/10.1175/MWR-D-22-0179.1

Howell, B., S. Egan, and C. Fine, 2022: Application of Microwave Space-Based Environmental Monitoring (SBEM) Data for Operational Tropical Cyclone Intensity Estimation at the Joint Typhoon Warning Center. *Bull. Amer. Meteor. Soc.*, **103**, E2315–E2322. https://doi.org/10.1175/BAMS-D-21-0180.1.

Huang, L., X. Li, B. Liu, J. A. Zhang, D. Shen, Z. Zhang, and W. Yu, 2018: Tropical cyclone boundary layer rolls in synthetic aperture radar imagery. *Journal of Geophysical Research: Oceans*, **123**, 2981-2996. https://doi.org/10.1029/2018JC013755

Huang, F., and co-authors, 2022: Assessment of FY-3E GNOS-II GNSS-R Global Wind Product. *IEEE Journal of Selected Topics in Applied Earth Observations and Remote Sensing,* **99**, 1-15. https://doi.org/10.1109/JSTARS.2022.3205331.

Huffman, G. J., Bolvin D. T. , Braithwaite D. , Hsu K. , Joyce R. , Kidd C. , Nelkin E. J. , and Xie P. , 2015: NASA Global Precipitation Measurement Integrated Multi-satellitE Retrievals for GPM (IMERG). Algorithm Theoretical Basis Doc., version 4.5, 30 pp. [Available online at http://pmm.nasa.gov/sites/default/files/document_files/IMERG_ATBD_V4.5.pdf.]

Ikuta, Y., and U. Shimada, 2024: Impact of Assimilation of the Tropical Cyclone Strong Winds Observed by Synthetic Aperture Radar on Analyses and Forecasts. *Mon. Wea. Rev.*, **152**, 1007–1025. https://doi.org/10.1175/MWR-D-23-0103.1.

Isoguchi O., T. Tadono, M. Ohki, U. Shimada, M. Yamaguchi, M. Hayashi, and W. Yanase, 2021: Hurricane Ocean Surface Wind Retrieval from ALOS-2 PALSAR-2 Cross-Polarized Measurements. *2021 IEEE International Geoscience and Remote Sensing Symposium IGARSS*, Brussels, Belgium, 7291-7294. https://doi.org/10.1109/IGARSS47720.2021.9554411.

Jackson, C. R., T. W. Ruff, J. A. Knaff, A. Mouche, and C. R. Sampson, 2021: Chasing cyclones from space. *Eos,* **102.** https://doi.org/10.1029/2021EO159148.

Jones, T. A., D. Cecil, and M. DeMaria, 2006: Passive-Microwave-Enhanced Statistical Hurricane Intensity Prediction Scheme. *Wea. Forecasting*, **21**, 613–635. https://doi.org/10.1175/WAF941.1.

Joyce, R. J., Janowiak J. E., Arkin P. A., and Xie P., 2004: CMORPH: A method that produces global precipitation estimates from passive microwave and infrared data at high spatial and temporal resolution. *J. Hydrometeor.*, **5**, 487–503. https://doi.org/10.1175/1525-7541

Kaplan, J., M. DeMaria, and J. A. Knaff, 2010: A Revised Tropical Cyclone Rapid Intensification Index for the Atlantic and Eastern North Pacific Basins. *Wea. Forecasting*, **25**, 220–241. https://doi.org/10.1175/2009WAF2222280.1.

Kerr, Y. H., et al., 2010: The SMOS Mission: new tool for monitoring key elements of the global water cycle. *Proc. IEEE,* **98**, 66e687. https://doi.org/ 10.1109/JPROC.2010.2043032.

Kidder, S. Q., M. D. Goldberg, R. M. Zehr, M. DeMaria, J. F. W. Purdom, C. S. Velden, N. C. Grody, and S. J. Kusselson, 2000: Satellite Analysis of Tropical Cyclones Using the Advanced Microwave Sounding Unit (AMSU). *Bull. Amer. Meteor. Soc.*, **81**, 1241–1260. https://doi.org/10.1175/1520-0477(2000)081<1241:SAOTCU>2.3.CO;2.

Kidder, S.Q. and A.S. Jones, 2007: A blended satellite Total Precipitable Water product for operational forecasting. *Journal of Atmospheric and Oceanic Tech.*, **24**, 74-81.

King, G. P., M. Portabella, W. Lin, and A. Stoffelen, 2022: Correlating Extremes in Wind Divergence with Extremes in Rain over the Tropical Atlantic. *Remote Sensing*, **14**(5), 1147. https://doi.org/10.3390/rs14051147

Kishimoto, K., M. Sasaki, and M. Kunitsugu, 2013: Cloud Grid Information Objective Dvorak Analysis (CLOUD) at the RSMC Tokyo - Typhoon Center. *Technical Review of RSMC Tokyo-Typhoon Center*, **13**, 1–15.

Knaff, J. A., D. P. Brown, J. Courtney, G. M. Gallina, and J. L. Beven, 2010: An Evaluation of Dvorak Technique–Based Tropical Cyclone Intensity Estimates. *Wea. Forecasting*, **25**, 1362–1379, https://doi.org/10.1175/2010WAF2222375.1.

Knaff, J. A., M. DeMaria, D. A. Molenar, C. R. Sampson, and M. G. Seybold, 2011: An automated, objective, multi-satellite platform tropical cyclone surface wind analysis. *J. of Applied Meteorology and Climatology.* **50(**10), 2149-2166. https://doi.org/10.1175/2011JAMC2673.1.

Knaff, J. A., S. P. Longmore, and D. A. Molenar, 2014: An Objective Satellite-Based Tropical Cyclone Size Climatology. *J. Climate*, **27**, 455–476. https://doi.org/10.1175/JCLI-D-13-00096.1.

Knaff, J. A., C. J. Slocum, and K. D. Musgrave, 2019: Quantification and Exploration of Diurnal Oscillations in Tropical Cyclones. *Mon. Wea. Rev.*, **147**(6), 2105-2121. https://doi.org/10.1175/MWR-D-18-0379.1.

Knaff, J.A., C. R. Sampson, M. Kucas, C. J. Slocum, M. J. Brennan, T. Meissner, L. Ricciardulli, A. Mouche, N. Reul, M. Morris, G. Chirokova, and P. Caroff, 2021: A practical guide to estimating tropical cyclone surface winds: History, current status, emerging technologies, and a look to the future. *Tropical Cyclone Research and Review*, **10**(3), 125-150. https://doi.org/10.1016/j.tcrr.2021.09.002.

Knaff, J. A., 2024: Using satellite derived motion winds to improve monitoring and forecasting of tropical cyclones. *36th AMS Conference on Hurricanes and Tropical Meteorology*, Long Beach, CA. https://ams.confex.com/ams/36Hurricanes/meetingapp.cgi/Paper/441208

Knutson, T. et al., 2019: Tropical cyclones and climate change assessment: Part I: Detection and attribution. *Bull. Am. Meteorol. Soc.* **100**, 1987–2007.

Knutson, T. et al., 2020: Tropical cyclones and climate change assessment: Part II. Projections. *Bull. Am. Meteorol. Soc.*, **94**, 231–245.

Knapp, K. and M. C. Kruk, 2010: Quantifying interagency differences in tropical cyclone best track wind speed estimates. *Mon. Weather Rev.* **138**, 1459–1473.

Knapp, K. R., M. C. Kruk, D. H. Levinson, and E. J. Gibney, 2009: Archive Compiles New Resource for Global Tropical Cyclone Research, *Eos Trans. AGU*, **90**(6), 46–66. doi:10.1029/2009EO060002.

Knapp, K. R., and Coauthors, 2011: Globally Gridded Satellite Observations for Climate Studies. *Bull. Amer. Meteor. Soc.*, **92**, 893–907. https://doi.org/10.1175/2011BAMS3039.1.

Knapp, K., C. S. Velden, and A. J. Wimmers, 2018: A global climatology of tropical cyclone eyes. *Mon. Weather Rev.* **146**, 2089–2101.

Kossin, J. P., T. L. Olander, and K. R. Knapp, 2013: Trend Analysis with a New Global Record of Tropical Cyclone Intensity. *J. Climate*, **26**, 9960–9976. https://doi.org/10.1175/JCLI-D-13-00262.1.

Kossin, J. P., 2015: Validating atmospheric reanalysis data using tropical cyclones as thermometers. *Bull. Amer. Meteor. Soc.*, **96**, 1089–1096. https://doi.org/10.1175/BAMS-D-14-00180.1.

Kossin, J., K. Knapp, T. Olander and C. Velden, 2020: Global increase in major tropical cyclone exceedance probability over the past four decades. PNAS, 117 (22) 11975-11980. https://doi.org/10.1073/pnas.1920849117

Kossin, J. P., D. C. Herndon, A. J. Wimmers, X. Guo, and E. S. Blake, 2023: M-PERC: A New Satellite Microwave-Based Model to Diagnose the Onset of Tropical Cyclone Eyewall Replacement Cycles. *Wea. Forecasting*, **38**, 1405–1411. https://doi.org/10.1175/WAF-D-22-0178.1.

Lagerquist, R., J. A. Knaff, C. J. Slocum, K. Musgrave, and I. Ebert-Uphoff, 2024: Identifying data sources and physical strategies used by neural networks to predict TC rapid intensification. *Wea. Forecasting*, in review.

Lagouvardos, K., Kotroni, V., Nickovic, S., Jovic, D., Kallos, G. and Tremback, C.J., 1999: Observations and model simulations of a winter sub-synoptic vortex over the central Mediterranean. *Met. Apps*, **6**, 371-383. https://doi.org/10.1017/S1350482799001309

Lagouvardos, K., Karagiannidis, A., Dafis, S., Kalimeris, A., Kotroni, V., 2022: Ianos—A Hurricane in the Mediterranean. *Bull. Am. Meteorol. Soc.*, **103**, E1621–E1636.

Lazzara, M. et al., 1999: The Man computer Interactive Data Access System: 25 Years of Interactive Processing, *Bulletin of the American Meteorological Society*, **80**, Number 2, 271–284.

Lee, J., J. Im, D.-H. Cha, H. Park, and S. Sim, 2020: Tropical cyclone intensity estimation using multi-dimensional convolutional neural networks from geostationary satellite data. *Remote Sens.*, **12**, 108. https://doi.org/10.3390/rs12010108.

Lewis, W.E.; Velden, C.S.; Stettner, D., 2020: Strategies for Assimilating High-Density Atmospheric Motion Vectors into a Regional Tropical Cyclone Forecast Model (HWRF). *Atmosphere*, **11**, 673. https://doi.org/10.3390/atmos11060673

Li, X. M., T. Zhang, B. Huang, T. Jia, 2018: Capabilities of Chinese Gaofen-3 synthetic aperture radar in selected topics for coastal and ocean observations. *Remote Sensing*, **10**, p. 1929. 10.3390/rs10121929

Li, J., J. Li., C. Velden, P. Wang, T. Schmit and J. Sippel, 2020: Impact of Rapid-Scan-Based Dynamical Information from GOES-16 on HWRF Hurricane Forecasts. *Journal of Geophysical Research: Atmospheres*, **125**, Issue 3, article id. e2019JD031647

Lim, A. H. N., Nebuda, S. E., Jung, J. A., Daniels, J. M., Bailey, A., Bresky, W., Bi, L., Mehra, A., 2022: Optimizing the Assimilation of the GOES-16/-17 Atmospheric Motion Vectors in the Hurricane Weather Forecasting (HWRF) Model. *Remote Sensing*, **14**(13), 3068. https://doi.org/10.3390/rs14133068

Liu S., C. Grassotti, Q. Liu, Y.-K. Lee, R. Honeyager, Y. Zhou and M. Fang, 2020: The NOAA Microwave Integrated Retrieval System (MiRS): Validation of Precipitation From Multiple Polar-Orbiting Satellites. *IEEE selected topics in applied Earth observations and remote sensing*, **13**, 3019-3031.

Lonfat, M., F. D. Marks, and S. Chen, 2004: Precipitation distribution in tropical cyclones using the Tropical Rainfall Measuring Mission (TRMM) Microwave Imager: A global perspective. *Mon. Wea. Rev.*, **132**, 1645–1660. https://doi.org/10.1175/1520-0493(2004)132<1645:PDITCU>2.0.CO;2.

Magnusson, L., and Co-authors, 2024: The role of observations in ECMWF tropical cyclone initialization and forecasting. Accepted in *QJRMS*.

Manaster, A., L. Ricciardulli, T. Meissner, 2021: Tropical cyclone winds from WindSat, AMSR2, and SMAP: comparison with the HWRF model. *Remote Sensing*, **13** (2021), 2347-2363. 10.3390/rs13122347

Marinescu, P., L. Cucurull, K. Apodoca, L. Bucci and I. Genkova, 2022: The characterization and impact of Aeolus wind profile observations in NOAA's regional tropical cyclone model (HWRF). *QJRMS*, **148**, 3491-3508. https://doi.org/10.1002/qj.4370

Marra, A.C., and Co-authors, 2019: The Precipitation Structure of the Mediterranean Tropical-Like Cyclone Numa: Analysis of GPM Observations and Numerical Weather Prediction Model Simulations. *Remote Sens.* **11**, 1690. https://doi.org/10.3390/rs11141690

Maturi, E., Harris, A., Mittaz, J., Sapper, J., Wick, G., Zhu, X., Dash, P. and Koner, P., 2017: A new high-resolution sea surface temperature blended analysis. *Bulletin of the American Meteorological Society*, **98** (5). pp. 1015-1026. ISSN 15200477. https://doi.org/10.1175/BAMS-D-15-00002.1

McNally, T., M. Bonavita, and J. Thépaut, 2014: The role of satellite data in the forecasting of Hurricane Sandy, *Mon. Weather Rev.*, **142**, 634–646.

Mecklenburg, S., and co-authors, 2016: ESA's Soil Moisture and Ocean Salinity mission: from science to operational applications. *Remote Sens. Environ.* **180**, 3e18. https://doi.org/10.1016/ j.rse.2015.12.025.

Meissner, T., L. Ricciardulli, and F. J. Wentz, 2017: Capability of the SMAP mission to measure ocean surface winds in storms. *Bull. Amer. Meteor. Soc*. **98**, 1660-1677. https://doi.org/10.1175/BAMS-D-16-0052.1.

Mercer A., Grimes A., 2017: Atlantic tropical cyclone rapid intensification probabilistic forecasts from an ensemble of machine learning methods. *Proc. Comput. Sci.,* **114**, 333–340. https://doi.org/10.1016/j.procs.2017.09.036

Miglietta, M., Laviola, S., Malvaldi, A., Conte, D., Levizzani, V., Price, C., 2013: Analysis of tropical-like cyclones over the Mediterranean Sea through a combined modeling and satellite approach. *Geophysical Research Letters,* **40**, 2400–2405.

Miglietta, M. M., D. Cerrai, S. Laviola, E. Cattani, and V. Levizzani, 2017: Potential vorticity patterns in Mediterranean "hurricanes". *Geophys. Res. Lett.*, **44**, 2537–2545. doi:10.1002/2017GL072670.

Miglietta M. M., R. Rotunno, 2019: Development mechanisms for Mediterranean tropical-like cyclones (medicanes). *Q J R Meteorol Soc.,* **145**, 1444–1460. https://doi.org/10.1002/qj.3503

Miller, B. I., 1958: On the maximum intensity of hurricanes. *J. Atmos. Sci.*, **15**, 184–195. https://doi.org/10.1175/1520-0469(1958)015<0184:OTMIOH>2.0.CO;2.

Miller, W., Y. Chen, S.-P Ho, and X. Shao, 2023: Evaluating the Impacts of COSMIC-2 GNSS RO Bending Angle Assimilation on Atlantic Hurricane Forecasts Using the HWRF Model. *Mon. Wea. Rev.*, **151**, 1821-1847.

Minamide, M., and F. Zhang, 2018: Assimilation of all-sky infrared radiances from Himawari-8 and impacts of moisture and hydrometer initialization on convection-permitting tropical cyclone prediction. *Mon. Wea. Rev.*, **146**, 3241–3258. https://doi.org/10.1175/MWR-D-17-0367.1.

Moore Torres, J. C., C. R. Jackson, T. W. Ruff, S. R. Helfrich, and R. Romeiser, 2023: Observing Tropical Cyclone Morphology Using RADARSAT-2 and Sentinel-1 Synthetic Aperture Radar Images. *J. Atmos. Oceanic Technol.*, **40**, 789–801. https://doi.org/10.1175/JTECH-D-22-0053.1.

Mouche, A., Chapron, B., Zhang, B., & Husson, R., 2017: Combined co- and cross-polarized SAR measurements under extreme wind conditions. *IEEE Xplore: IEEE Transactions on Geoscience and Remote Sensing*, **55**, 6476–6755.

Mouche, A., B. Chapron, J. A. Knaff, Y. Zhao, B. Zhang, and C. Combot, 2019: Co-polarized and cross-polarized SAR measurements for high-resolution description of major hurricane wind structures: Application to Irma category 5 hurricane. *J. Geophys. Res. Oceans*, **124**(6), 3905-3922. https://doi.org/10.1029/2019JC015056.

Ni, W.; Stoffelen, A., Ren, K., Yang, X., Vogelzang, J., 2022: SAR and ASCAT Tropical Cyclone Wind Speed Reconciliation. *Remote Sens.* **14**, 5535. https://doi.org/10.3390/rs14215535

Ni, W., A. Stoffelen and co-authors, 2024: Enhanced Tropical Cyclone ASCAT Winds Guided by SAR-Learned Spatial Structure Functions, *IEEE Transactions on Geoscience and Remote Sensing*, vol. 63, pp. 1-19, 2025, Art no. 4100719, https://doi.org/10.1109\\TGRS.2024.3516209.

NOAA/NESDIS, 2024: Update on GOES/POES/Non NOAA Satellites. [available on-line at https://www.weather.gov/media/tropical/IHC-2024-Presentations/Fiore-Aiwu-li-NESDIS-.pdf] Last accessed 11/26/2024.

Nolan, D. S., and M. T. Montgomery, 2000: The Algebraic Growth of Wavenumber One Disturbances in Hurricane-Like Vortices. *J. Atmos. Sci.*, **57**, 3514–3538. https://doi.org/10.1175/1520-0469(2000)057<3514:TAGOWO>2.0.CO;2.

Nonaka, K., K. Shimoji, and K. Kato, 2016: Estimation of the Sea Surface Winds in the Vicinity of Typhoons using Himawari-8 Low-Level AMVs. *Proc. 13th International Winds Workshop*, Monterey, California, USA. https://cimss.ssec.wisc.edu/iwwg/iww13/proceedings_iww13/papers/session6/IWW13_Session6_4_Nonaka_final_update.pdf.

Okabe, I., K. Okamoto, 2024: Impact of Aeolus horizontal line-of-sight wind observations on tropical cyclone forecasting in a global numerical weather prediction system. *QJRMS*, **150**. https://doi.org/10.1002/qj.4653.

Olander, T. L., and Velden C. S., 2007: The Advanced Dvorak Technique: Continued development of an objective scheme to estimate tropical cyclone intensity using geostationary infrared satellite imagery. *Wea. Forecasting*, **22,** 287–298.

Olander, T. L., and C. S. Velden, 2009: Tropical Cyclone Convection and Intensity Analysis Using Differenced Infrared and Water Vapor Imagery. *Wea. Forecasting*, **24**, 1558–1572. https://doi.org/10.1175/2009WAF2222284.1.

Olander, T. L., and C. S. Velden, 2019: The Advanced Dvorak Technique (ADT) for Estimating Tropical Cyclone Intensity: Update and New Capabilities. *Wea. Forecasting*, **34**, 905–922. https://doi.org/10.1175/WAF-D-19-0007.1.

Olander, T., A. Wimmers, C. Velden, and J. P. Kossin, 2021: Investigation of Machine Learning Using Satellite-Based Advanced Dvorak Technique Analysis Parameters to Estimate Tropical Cyclone Intensity. *Wea. Forecasting*, **36**, 2161–2186, https://doi.org/10.1175/WAF-D-20-0234.1.

Oyama, R., 2014: Estimation of tropical cyclone central pressure from warm core intensity observed by the Advanced Microwave Sounding Unit-A (AMSU-A). *Papers in Meteorology and Geophysics*, **65**, 35-56. https://doi.org/10.2467/mripapers.65.35

Panegrossi, G., D'Adderio, L.P., Dafis, S., Rysman, J.-F., Casella, D., Dietrich, S., Sanò, P., 2023: Warm Core and Deep Convection in Medicanes: A Passive Microwave-Based Investigation. *Remote Sens.* **15**, 2838. https://doi.org/10.3390/rs15112838

Polverari, F., M. Portabella, W. Lin, J.W. Sapp, A. Stoffelen, Z. Jelenak, P.S. Chang, 2022: On high and extreme wind calibration using ASCAT. *IEEE Trans. Geosci. Remote Sensing*, **60**, pp. 1-10. 10.1109/TGRS.2021.3079898

Portabella, M., A.S. Rabaneda, and G. Grieco, 2022: MAXSS: Algorithm Theoretical Baseline Document for SFMR-based Satellite-derived Extreme Wind Recalibration. http://hdl.handle.net/10261/287615

Pradhan, R., R. Aygun, M. Maskey, R. Ramachandran, and D. Cecil, 2018: Tropical cyclone intensity estimation using a deep convolutional neural network. *IEEE Trans. Image Process.*, **27**, 692–702. https://doi.org/10.1109/TIP.2017.2766358.

Qian, B., H. Jiang, F. Weng, and Y. Wu, 2020: Climatology of Passive Microwave Brightness Temperatures in Tropical Cyclones and their Relations to Storm Intensities as seen by FY-3B/MWRI. *Remote Sensing*, **12**(1), 147. https://doi.org/10.3390/rs12010147.

Razin, M.N., C. J. Slocum, J. A. Knaff, P. J. Brown and M. M. Bell, 2023: Tropical Cyclone Precipitation, Infrared, Microwave, and Environmental Dataset (TC PRIMED). *Bull. Amer. Meteor. Soc.*, **104**, E1980-E1998. https://doi.org/10.1175/BAMS-D-21-0052.1.

Reale, O., and R. Atlas, 2001: Tropical Cyclone–Like Vortices in the Extratropics: Observational Evidence and Synoptic Analysis. *Wea. Forecasting*, **16**, 7–34. https://doi.org/10.1175/1520-0434(2001)016<0007:TCLVIT>2.0.CO;2

Reul, N., B. Chapron, E. Zabolotskikh, C. Donlon, A. Mouche, J. Tenerelli, F. Collard, J. F. Piolle, A. Fore, S. Yueh, J. Cotton, P. Francis, Y. Quilfen, and V. Kudryavtsev, 2017: A new generation of tropical cyclone size measurements from space. *Bull. Amer. Meteor. Soc.*, **98**, 2367-2385. https://doi.org/10.1175/BAMS-D-15-00291.1.

Ricciardulli, L., C. Mears, A. Manaster, T. Meissner, 2021: Assessment of CYGNSS wind speed retrievals in tropical cyclones. *Remote Sensing*, **13**, p. 5110. 10.3390/rs13245110

Ricciardulli, L., A. Manaster, 2021: Intercalibration of ASCAT scatterometer winds from MetOp-A, -B, and -C, for a stable climate data record. *Remote Sensing*, **13**, p. 3678. 10.3390/rs13183678

Ricciardulli, L., and Coauthors, 2023: Remote sensing and analysis of tropical cyclones: Current and emerging satellite sensors. *Tropical Cyclone Research and Review*, **12**, Issue 4, 267-293, ISSN 2225-6032. https://doi.org/10.1016/j.tcrr.2023.12.003.

Ritchie, E. A., G. Valliere-Kelley, M. F. Piñeros, and J. S. Tyo, 2012: Tropical cyclone intensity estimation in the North Atlantic basin using an improved deviation angle variance technique. *Wea. Forecasting*, **27**, 1264–1277. https://doi.org/10.1175/WAF-D-11-00156.1.

Rostan, F., D. Ulrich, S. Riegger and A. Østergaard, 2016: MetoP-SG SCA wind scatterometer design and performance. *2016 IEEE International Geoscience and Remote Sensing Symposium (IGARSS)*, Beijing, China, pp. 7366-7369. https://doi.org/10.1109/IGARSS.2016.7730921.

Ruf, C., C. Chew, T. Lang, M.G. Morris, K. Nave, A. Ridley, R. Balasubramaniam, 2018: A new paradigm in earth environmental monitoring with the CYGNSS small satellite constellation. *Sci. Rep*., **8**, p. 8782, 10.1038/s41598-018-27127-4

Ruf, C., S. Gleason, D.S. McKague, 2019: Assessment of CYGNSS wind speed retrieval uncertainty. *IEEE J. Sel. Top. Appl. Earth Observations Remote Sensing*, **12**, pp. 87-97, 10.1109/JSTARS.2018.2825948

Ryglicki, D. R., J. D. Doyle, D. Hodyss, J. H. Cossuth, Y. Jin, K. C. Viner, and J. M. Schmidt, 2019: The Unexpected Rapid Intensification of Tropical Cyclones in Moderate Vertical Wind Shear. Part III: Outflow–Environment Interaction. *Mon. Wea. Rev.*, **147**, 2919–2940. https://doi.org/10.1175/MWR-D-18-0370.1.

Ryglicki, D., C. S. Velden, P. D. Reasor, D. Hodyss, and J. D. Doyle, 2021: Observations of atypical rapid intensification characteristics in Hurricane Dorian (2019). *Mon. Wea. Rev*, **149**, 2131–2150. https://doi.org/10.1175/MWR-D-20-0413.1.

Rysman, J-F., C. Claud, and S. Dafis, 2021: Global monitoring of deep convection using passive microwave observations. *Atmo. Res*., **247**. https://doi.org/10.1016/j.atmosres.2020.105244.

Said, F., Z. Jelenak, J. Park, P.S. Chang, 2021: The NOAA track-wise wind retrieval algorithm and product assessment for CyGNSS. *IEEE Trans. Geosci. Remote Sensing*, pp. 1-24. 10.1109/TGRS.2021.3087426

Sampson, C.R., J. Cummings, J. A. Knaff, M. DeMaria, and E. A. Serra, 2022: An upper ocean thermal field metrics dataset. *Meteor.*, **1**, 327–340. https://doi.org/10.3390/meteorology1030021

Sampson, C. R., J. A. Knaff, C. J. Slocum, M. J. Onderlinde, A. Brammer, M. Frost, and B. Strahl, 2023: Deterministic rapid intensity forecast guidance for the Joint Typhoon Warning Center's area of Responsibility. *Wea. Forecasting*, **38**, 2631–2640. https://doi.org/10.1175/WAF-D-23-0084.1.

Sawada, M., Z. Ma, A. Mehra, V. Tallapragada, R. Oyama, and K. Shimoji, 2019: Impacts of Assimilating High-Resolution Atmospheric Motion Vectors Derived from Himawari-8 on Tropical Cyclone Forecast in HWRF. *Mon. Wea. Rev.*, **147**, 3721–3740. https://doi.org/10.1175/MWR-D-18-0261.1.

Sawada, M., Z. Ma, A. Mehra, V. Tallapragada, R. Oyama, K. Shimoji, 2020: Assimilation of Himawari-8 Rapid-Scan Atmospheric Motion Vectors on Tropical Cyclone in HWRF System. *Atmosphere*, **11**, 601. https://doi.org/10.3390/atmos11060601

Schreck III, C., K. R. Knapp, J. P. Kossin, 2014: The impact of best track discrepancies on global tropical cyclone climatologies using IBTrACS. *Mon. Weather Rev.* **142**, 3881–3899.

Shay L., Goni G., Black P., 2000: Effects of a warm oceanic feature on Hurricane Opal. *Mon. Weather Rev*., **128**, 1366–1383.

Sheets, R. C., 1990: The National Hurricane Center-Past, Present, and Future. *Wea. Forecasting*, **5**, 185–232. https://doi.org/10.1175/1520-0434(1990)005<0185:TNHCPA>2.0.CO;2.

Shibata, A., 2006: A wind speed retrieval algorithm by combining 6 and 10 GHz data from Advanced Microwave Scanning Radiometer: wind speed inside hurricanes. *J. Oceanogr*., **62**, pp. 351-359. 10.1007/s10872-006-0060-8

Shimada, U., M. Hayashi, and A. Mouche, 2024: A comparison between SAR wind speeds and western North Pacific tropical cyclone best track estimates. *J. Meteor. Soc. Japan*, **102.** http://doi:10.2151/jmsj.2024-031.

Sitkowski, M., J. P. Kossin, and C. M. Rozoff, 2011: Intensity and structure changes during hurricane eyewall replacement cycles. *Mon. Wea. Rev*., **139**, 3829–3847.

Slocum, C. J., J. A. Knaff, and S. N. Stevenson, 2023: Lightning-Based Tropical Cyclone Rapid Intensification Guidance. *Wea. Forecasting*, **38**, 1209-1227. https://doi.org/10.1175/WAF-D-22-0157.1.

Slocum, C.J., J.A. Knaff, and C. R. Sampson, 2024: A Forest-based Rapid Intensification Aid for Tropical Cyclones. *Artificial Intelligence for the Earth Systems*, in review.

Sobel, A. et al., 2016: Human influence on tropical cyclone intensity. *Science* **353**, 242–246.

Soisuvarn, S., Z. Jelenak, P.S. Chang, S.O. Alsweiss, Q. Zhu, 2013: CMOD5.H-a high wind geophysical model function for C-band vertically polarized satellite scatterometer measurements. *IEEE Trans. Geosci. Remote Sensing*, **51**, pp. 3744-3760. 10.1109/TGRS.2012.2219871

Stettner, D., Velden, C., Rabin, R., Wanzong, S., Daniels, J., & Bresky, W., 2019: Development of enhanced vortex-scale atmospheric motion vectors for hurricane applications. *Remote Sensing*, **11**, 1981. https://doi.org/10.3390/rs11171981

Stoffelen, A. A. Mouche, F. Polverari, G.-J. van Zadelhoff, J. Sapp, M. Portabella, P. Chang, W. Lin, and Z. Jelenak, 2020: C-band High and Extreme-Force Speeds (CHEFS)-Final Report, Available: www.eumetsat.int/CHEFS.

Stoffelen A, Marseille G-J, Ni W, et al. 2021: Hurricane ocean wind speeds. *Proc. IEEE International Geoscience and Remote Sensing Symposium IGARSS*, 1182–1185.

Straume, A.G., et al., 2020: ESA's space-based Doppler wind Lidar Mission Aeolus: first wind and aerosol product assessment results. *EPJ Web of Conferences,* **237***,* 01007, Oberpfaffenhofen, Germany. https://doi.org/10.1051/epjconf/202023701007

Su, H., L. Wu, J., H. Jiang, R. Pai, A. Liu, A., J. Zhai, P. Tavallali, and M. DeMaria, 2020: Applying satellite observations of tropical cyclone internal structures to rapid intensification forecast with machine learning. *Geophys. Res. Lett.*, **47**, e2020GL089102. https://doi.org/10.1029/2020GL089102.

Subrahmanyam, K. V., R. V. Bothale, M. Swapna, and P. Chauhan, 2023: Deciphering the signatures of oceanic convective rain cells using simultaneous observations from C-band synthetic aperture radar onboard EOS-04 satellite and GPM measurements. *Geophysical Research Letters*, **50**, e2022GL102317. https://doi.org/10.1029/2022GL102317

Sun, Y., and co-authors, 2023: GNOS-II on Fengyun-3 Satellite Series: Exploration of Multi-GNSS Reflection Signals for Operational Applications. *Remote Sensing*, **15**(24), 5756. https://doi.org/10.3390/rs15245756

Tsujino, S., Horinouchi, T., Tsukada, T., Kuo, H.-C., Yamada, H., & Tsuboki, K., 2021: Inner-core wind field in a concentric eyewall replacement of Typhoon Trami (2018): A quantitative analysis based on the Himawari-8 satellite. *Journal of Geophysical Research: Atmospheres*, **126**(7). https://doi.org/10.1029/2020JD034434

Tsukada, T., and T. Horinouchi, 2020: Estimation of the tangential winds and asymmetric structures in typhoon inner core region using Himawari-8. *Geophys. Res. Lett.*, **47.** https://doi.org/10.1029/2020GL087637.

Tsukada, T., and T. Horinouchi, 2023: Strong Relationship between Eye Radius and Radius of Maximum Wind of Tropical Cyclones. *Mon. Wea. Rev.*, **151**, 569–588. https://doi.org/10.1175/MWR-D-22-0106.1.

Tsukada, T., T. Horinouchi, and S. Tsujino, 2024: Wind Distribution in the Eye of Tropical Cyclone Revealed by a Novel Atmospheric Motion Vector Derivation. *JGR Atmospheres*, **129**, e2023JD040585. https://doi.org/10.1029/2023JD040585.

Tuell, J.P, R. K. Henry, J. D. Lawson, F. P. Griffith, 2008: The Evolution of AWIPS – Progress, Future Plans and Status. *Proc. 24th Conf. on IIPS,* Amer. Meteor. Soc., 6A.1.

Velden, C. S., Olander T. L., and Zehr R. M., 1998: Development of an objective scheme to estimate tropical cyclone intensity from digital geostationary satellite infrared imagery. *Wea. Forecasting*, **13,** 172–186.

Velden, C. S., and Coauthors, 2006: Supplement to: The Dvorak tropical cyclone intensity estimation technique: A satellite-based method that has endured for over 30 years. *Bull. Amer. Meteor. Soc.*, **87,** (Suppl.). S6–S9. doi:10.1175/BAMS-87-9-Velden.

Velden, C., W. E. Lewis, W. Bresky, D. Stettner, J. Daniels, and S. Wanzong, 2017: Assimilation of High-Resolution Satellite-Derived Atmospheric Motion Vectors: Impact on HWRF Forecasts of Tropical Cyclone Track and Intensity. *Mon. Wea. Rev.*, **145**, 1107–1125. https://doi.org/10.1175/MWR-D-16-0229.1.

Velden, C. and D. Stettner, 2018: Improved Monitoring of the Evolving Upper-Tropospheric Wind Fields Over the Core of Tropical Cyclones Aided by High Spatiotemporal Resolution GOES-16 Atmospheric Motion Vectors. *Proc. 33rd Conf. Hurr. Trop. Meteor.*, Amer. Meteor. Soc., P245.

Velden, C. S., and D. Herndon, 2020: A Consensus Approach for Estimating Tropical Cyclone Intensity from Meteorological Satellites: SATCON. *Wea. Forecasting*, **35**, 1645–1662. https://doi.org/10.1175/WAF-D-20-0015.1.

Vinour, L., S. Jullien, A. Mouche, C. Combot, and M. Mangeas, 2021: Observations of Tropical Cyclone Inner-Core Fine-Scale Structure, and Its Link to Intensity Variations. *J. Atmos. Sci.*, **78**, 3651–3671. https://doi.org/10.1175/JAS-D-20-0245.1.

Wang, H., J. Zhu, M. Lin, Y. Zhang, Y. Chang, 2020: Evaluating Chinese HY-2B HSCAT Ocean Wind products using Buoys and other scatterometers. *IEEE Geosci. Remote Sensing Lett.,* **17**, pp. 923-927. 10.1109/LGRS.2019.2940384

Wang, Z., J. Zou, A. Stoffelen, W. Lin, A. Verhoef, X. Li, Y. He, Y. Zhang, M. Lin, 2021: Scatterometer sea-surface wind product validation for HY-2C. *IEEE J. Sel. Top. Appl. Earth Observations Remote Sensing*, **14**, pp. 6156-6164. 10.1109/JSTARS.2021.3087742

Wimmers, A. and C. Velden, 2007: MIMIC: A new approach to visualizing satellite microwave imagery of tropical cyclones. *Bull. Amer. Meteor. Soc*., **88**, pp.1187-1196.

Wimmers, A. and C. Velden, 2010: Objectively Determining the Rotational Center of Tropical Cyclones in Passive Microwave Satellite Imagery. *Journal of Applied Meteorology and Climatology,* **49**(9). https://doi.org10.1175/2010JAMC2490.1

Wimmers, A. J., C. S. Velden, 2011: Seamless Advective Blending of Total Precipitable Water Retrievals from Polar-Orbiting Satellites. *J. Appl. Meteor. Climatol*., **50**, 1024-1036. https://doi.org/10.1175/2010JAMC2589.1

Wimmers, A., C. Velden, and J. H. Cossuth, 2019: Using Deep Learning to Estimate Tropical Cyclone Intensity from Satellite Passive Microwave Imagery. *Mon. Wea. Rev.*, **147**, 2261–2282. https://doi.org/10.1175/MWR-D-18-0391.1.

Wimmers, A. J., S. Griffin, and C. Velden, 2024: A U-Net Retrieval of Tropical Cyclone Inner-Core Wind Fields from Microwave and Infrared Satellite Imagery. *Artif. Intell. Earth Syst.*, **3**, e230084. https://doi.org/10.1175/AIES-D-23-0084.1.

Wimmers, A., 2025: TC-CORE Quick Guide. https://tropic.ssec.wisc.edu/real-time/norm_tc-core/about/about.html (last accessed, March 2025).

Wingo, M. T., and D. J. Cecil, 2010: Effects of vertical wind shear on tropical cyclone precipitation. *Mon. Wea. Rev.*, **138**, 645–662. https://doi.org/10.1175/2009MWR2921.1.

WMO, 2024a: World Meteorological Organization Satellite Programme: Weather System Follow-on. https://space.oscar.wmo.int/satelliteprogrammes/view/wsf

WMO, 2024b: INFCOM-3 assesses core satellite data needs. https://wmo.int/media/update/infcom-3-assesses-core-satellite-data-needs

WMO, 2025: World Meteorological Organization Satellite Programme: Gap Analysis. https://space.oscar.wmo.int/gapanalyses?mission=12

Wu, T. C., H. Liu, S. Majumdar, C. Velden, and J. Anderson, 2014: Influence of assimilating satellite-derived atmospheric motion vector observations on numerical analyses and forecasts of tropical cyclone track and intensity. *Mon. Wea. Rev.*, **142**, 49–71. https://doi.org/10.1175/MWR-D-13-00023.1.

Wu, X.; Liu, Y.; Liu, S.; Jin, Y.; Xu, H., 2024: Assessment of Satellite Products in Estimating Tropical Cyclone Remote Precipitation over the Yangtze River Delta Region. *Atmosphere* **2024**, *15*, 667. https://doi.org/10.3390/atmos15060667

Xu W., Balaguru K., August A., Lalo N., Hodas N., DeMaria M., et al., 2021: Deep learning experiments for tropical cyclone intensity forecasts. *Weather Forecasting,* **36** (4), 1453–1470. https://doi.org/10.1175/WAF-D-20-0104.1

Yamaguchi, M., H. Owada, U. Shimada, M. Sawada, T. Iriguchi, K. D. Musgrave, and M. DeMaria, 2018: Tropical cyclone intensity prediction in the western North Pacific basin using SHIPS and JMA/GSM. *Scientific Online Letters on the Atmosphere (SOLA)*, **14**, 138-143. https://doi.org/10.2151/sola.2018-024

Yang, S., V. Lao, R. Bankert, T. R. Whitcomb, and J. Cossuth, 2021: Improved Climatology of Tropical Cyclone Precipitation from Satellite Passive Microwave Measurements. *J. Climate*, **34**, 4521–4537. https://doi.org/10.1175/JCLI-D-20-0196.1.

Yang, S.; Zhang, L.; Lin, M.; Zou, J.; Mu, B.; Peng, H., 2023: Evaluation of Sea Surface Wind Products from Scatterometer Onboard the Chinese HY-2D Satellite. *Remote Sens.* **15**, 852. https://doi.org/10.3390/rs15030852

Zawislak, J., and E. J. Zipser, 2010: Observations of seven African easterly waves in the east Atlantic during 2006. *J. Atmos. Sci.*, **67**, 26–43. https://doi.org/10.1175/2009JAS3118.1.

Zehr, R., 1989: Improving objective satellite estimates of tropical cyclone intensity. *Preprints 18th Conf. on Hurr. Trop. Meteor.,* San Diego, CA, Amer. Meteor. Soc., J25–J28.

Zhang, F., M. Minamide, and E. E. Clothiaux, 2016: Potential impacts of assimilating all-sky infrared satellite radiances from GOES-R on convection-permitting analysis and prediction of tropical cyclones. *Geophys. Res. Lett.*, **43**, 2954–2963. https://doi.org/10.1002/2016GL068468.

Zhang, F., M. Minamide, R. G. Nystrom, X. Chen, S. Lin, and L. M. Harris, 2019: Improving Harvey Forecasts with Next-Generation Weather Satellites: Advanced Hurricane Analysis and Prediction with Assimilation of GOES-R All-Sky Radiances. *Bull. Amer. Meteor. Soc.*, **100**, 1217–1222. https://doi.org/10.1175/BAMS-D-18-0149.1.

Zhang, P., and co-authors, 2023: FY-3G Satellite Instruments and Precipitation Products: First Report of China's Fengyun Rainfall Mission In-Orbit. *J Remote Sens.* **3***, p. 97.* DOI:10.34133/remotesensing.0097

Zhao, Y.; Zhao, C.; Sun, R.; Wang, Z., 2016: A Multiple Linear Regression Model for Tropical Cyclone Intensity Estimation from Satellite Infrared Images. *Atmosphere, 7*, 40. https://doi.org/10.3390/atmos7030040.

Zhuo, J., and Z. Tan, 2021: Physics-Augmented Deep Learning to Improve Tropical Cyclone Intensity and Size Estimation from Satellite Imagery. *Mon. Wea. Rev.*, **149**, 2097–2113. https://doi.org/10.1175/MWR-D-20-0333.1.

Zimbo, F.; Ingemi, D.; Guidi, G., 2022: The Tropical-like Cyclone "Ianos" in September 2020. *Meteorology*, **1**, 29-44. https://doi.org/10.3390/meteorology1010004